NASA CONTRACTOR REPORT

NASA CR-2405

NASA CR-2405

DIFFRACTION BY A PERFECTLY CONDUCTING RECTANGULAR CYLINDER WHICH IS ILLUMINATED BY AN ARRAY OF LINE SOURCES

by R. G. Kouyoumjian and N. Wang

Prepared by
THE OHIO STATE UNIVERSITY
ELECTROSCIENCE LABORATORY
Columbus, Ohio 43212
for Langley Research Center

NATIONAL AERONAUTICS AND SPACE ADMINISTRATION • WASHINGTON, D. C. • JUNE 1974

1. Report No.	2. Government Accession No.	3. Recipient's Catalog No.
NASA CR- 2405		

4. Title and Subtitle	5. Report Date
DIFFRACTION BY A PERFECTLY CONDUCTING RECTANGULAR CYLINDER WHICH IS ILLUMINATED BY AN ARRAY OF LINE SOURCES	June 1974
	6. Performing Organization Code
7. Author(s)	8. Performing Organization Report No.
R. G. Kouyoumjian and N. Wang	TR 3001-7
	10. Work Unit No.
9. Performing Organization Name and Address	502-33-13-02
The Ohio State University ElectroScience Laboratory Columbus, Ohio 43212	11. Contract or Grant No. NGR 36-008-144
	13. Type of Report and Period Covered
12. Sponsoring Agency Name and Address	Contractor Report
National Aeronautics and Space Administration Washington, D.C. 20546	14. Sponsoring Agency Code

15. Supplementary Notes

Topical report.

16. Abstract

The geometrical theory of diffraction (GTD) is employed to analyze the radiation from a perfectly-conducting rectangular cylinder illuminated by an array of line sources. The excitation of the cylinder by a single electric or magnetic current line source is considered first, and a solution which includes contributions from the geometrical optics rays and all singly- and doubly-diffracted rays is obtained. A new diffraction coefficient valid in the transition regions of the shadow and reflection boundaries is employed to obtain a continuous total field, except for negligible discontinuities in the doubly-diffracted field at its shadow boundaries. Patterns calculated by the GTD method are found to be in excellent agreement with those calculated from an integral equation formulation. Using superposition the solution for array or aperture excitation of the rectangular cylinder is obtained. A computer program for this solution is included.

17. Key Words (Suggested by Author(s))	18. Distribution Statement
Antenna, Spacecraft and Aircraft Antennas Applied Electromagnetic Theory	Unclassified - Unlimited STAR Category 09

19. Security Classif. (of this report)	20. Security Classif. (of this page)	21. No. of Pages	22. Price*
Unclassified	Unclassified	71	$3.75

*For sale by the National Technical Information Service, Springfield, Virginia 22151

Page Intentionally Left Blank

TABLE OF CONTENTS

I. INTRODUCTION

In this report the geometrical theory of diffraction (GTD) [1] is used to treat the diffraction by a perfectly-conducting rectangular cylinder which is illuminated by an array of electric or magnetic current line sources. The illumination by a single line source of the array is considered first with the geometry of the problem shown in Fig. 1. The scattered and total fields are calculated at all points exterior to the rectangular cylinder, except for the shaded regions around the source and edges, which are excluded because of the nature of the high-frequency approximation. More will be said about this later. The solution is then generalized to calculate the field of linear arrays of such line sources radiating in the presence of the cylinder.

The scattering by a rectangular cylinder has been considered previously for the special case of plane wave incidence. Mei and VanBladel [2,3] formulated the problem in terms of an integral equation which they solved numerically to find the surface currents on the rectangular cylinder. They give radiation patterns, scattering cross sections, and surface currents for both E- and H-polarized incident waves. There are two disadvantages associated with this method: 1) as the frequency increases, difficulties are encountered with the convergence of the solution (this is particularly true when the technique is employed to solve a three-dimensional scattering problem), 2) the solution provides no physical insight into the scattering mechanism. Morse [4] also studied this problem using the ordinary GTD to obtain expressions for the diffracted field away from shadow and reflection boundaries. Since the ordinary theory fails at shadow and reflection boundaries, he introduced supplementary solutions there. He employed Oberhettinger's uniform asymptotic solution [5] near the boundaries of the incident and reflected fields, and he employed an integral representation of the field near the shadow boundaries of the fields of the diffracted rays. Thus, he did not obtain a compact high-frequency solution to this problem. The difficulties encountered by Morse at these boundaries may be overcome with a new edge diffraction coefficient derived by Kouyoumjian and Pathak [6,7]. This diffraction coefficient can be applied in the transition regions adjacent to the shadow and reflection boundaries so that one obtains a total field which is valid and continuous everywhere away from edges and caustics. Their diffraction coefficient is employed in this analysis.

Using Keller's Generalized Fermat's Principle, we include contributions to the total field from the geometrical optics fields (incident and reflected), as well as singly-diffracted fields which appear to emanate from the edges. Doubly-diffracted fields have also been included to describe the interactions between the edges; however, multiply-diffracted rays of higher order have been neglected because, in general, their fields contribute insignificantly, for the problem defined here. The incident, reflected and diffracted rays may be shadowed in the geometrical optics sense, and hence they contribute to the total field only in their respective regions of illumination. Discontinuities in the

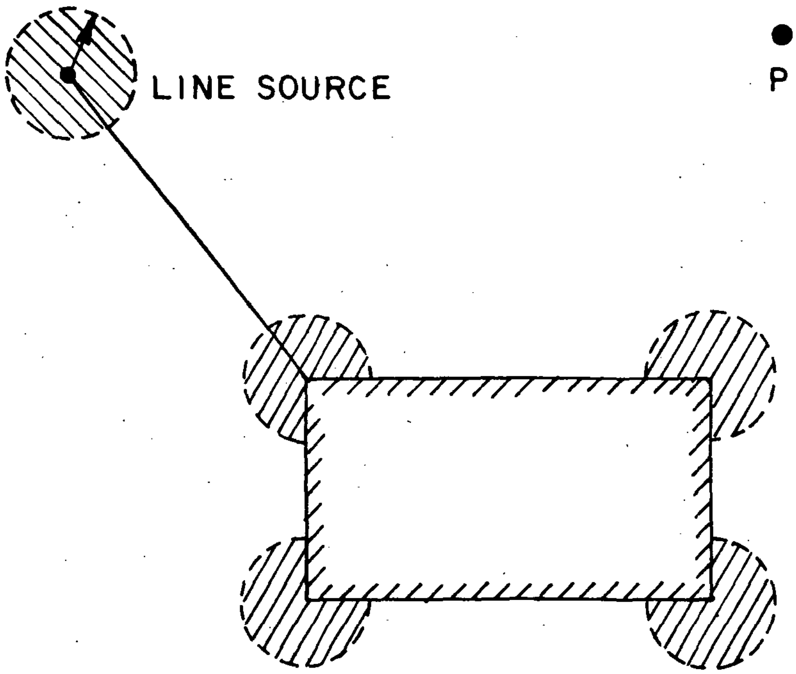

Fig. 1. Line source in the presence of the rectangular cylinder.

field are introduced at shadow boundaries and at the reflection boundaries, but they are symstematically removed by employing the new diffraction coefficient for the edge diffracted field mentioned previously. It should be pointed out that there are some residual discontinuities due to uncompensated discontinuities in the field of the doubly-diffracted rays at their shadow boundaries. However, these discontinuities are so small that they are not apparent in the plotted patterns. The patterns calculated from our GTD solution are found to be in excellent agreement with those calculated from numerical solutions.

Due to the high-frequency approximations of the incident and diffracted fields, our solution is restricted so that the following distances are greater than 0.7 wavelength.

1) The distance between the line source and the closest edge of the rectangular cylinder,

2) the distance between the observation point P and the closest edge of the rectangular cylinder,

3) the distances between the edges of the rectangular cylinder,

4) the distance between the observation point P and the closest line source, when calculating the incident or total fields.

A computer program based on the GTD solution for the rectangular cylinder in the presence of an array source has been written and is included in the report. With this program, it is possible to obtain numerical results for both the near- and far-fields of the cylinder under quite general conditions of illumination. Thus, the program is directly relevant to both antenna and scattering problems. As an example of its versatility, one notes that the program may be used to compute the pattern of an array of magnetic line sources mounted directly on the rectangular cylinder, provided the sources are not too close to an edge.

II. METHOD OF SOLUTION

Keller's geometrical theory of diffraction [1] is an extension of geometrical optics in which diffracted rays are introduced by a generalization of Fermat's principle, the excitation of the diffracted field is treated as a local phenomenon, and away from the diffracting surface the behavior of the diffracted field along its ray is the same as that of the geometrical optics field. The basic idea of GTD is that the field of the line source illuminates the rectangular cylinder giving rise to a reflected field and an edge diffracted field, which consists of the fields of singly and multiply-diffracted rays. The total field U(P) at a point P is equal to the sum of the fields on all rays through P.

$$U(P) = \sum_{\text{rays}} U_i(P) \tag{1}$$

which includes the incident field if P is not in the shadow region. The wave function U(P) represents a magnetic field parallel to the edge in case of a magnetic line source, and an electric field parallel to the edge in the case of an electric current line source. The pertinent rays and their associated fields will be discussed briefly in the following paragraphs.

A. Geometrical Optics Rays - Direct and Reflected

Let us consider the field radiated from a line source at O and observed at P as shown in Fig. 2. Fermat's principle predicts only the direct ray OP. If a line source is being considered, the field along OP is given by

$$U^i(P) = C \frac{e^{-jks_0}}{\sqrt{s_0}} , \tag{2}$$

where s_0 is the distance between O and P, and C is a conveniently chosen normalization constant. For the configuration shown in Fig. 2, the space surrounding the right-angle wedge may be divided into three regions:

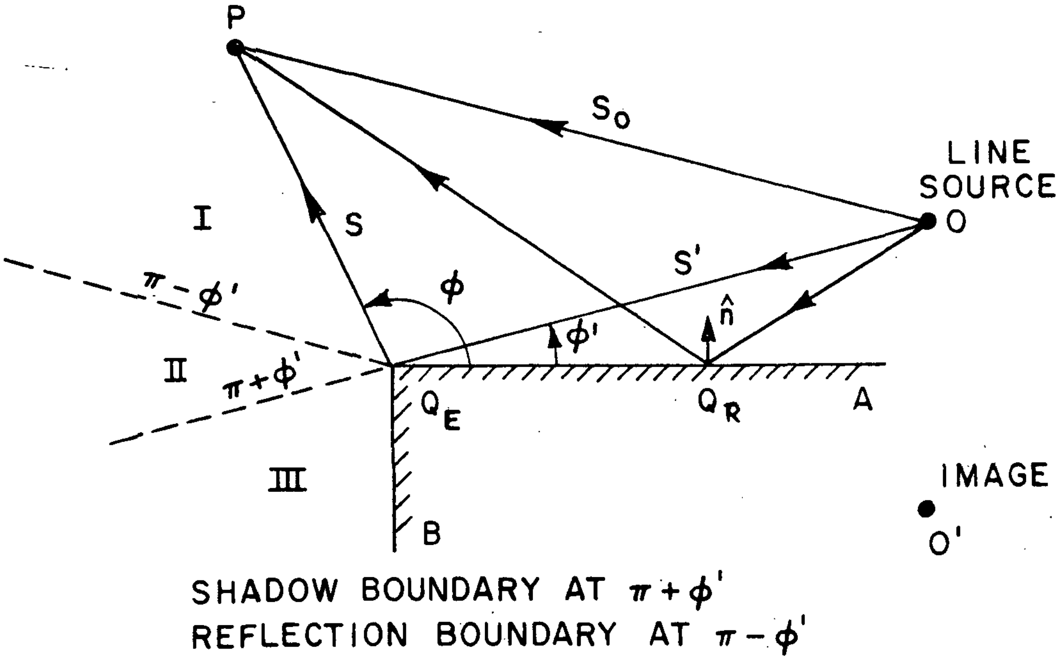

Fig. 2. Line source in the presence of a wedge.

Region I	$0 \leq \phi < \pi - \phi'$,
Region II	$\pi - \phi' < \phi < \pi + \phi'$,
Region III	$\pi + \phi' < \phi < 3\pi/2$.

Region III is the shadow region, which is not penetrated by the incident ray; the incident field vanishes here.

We know that there is a field reflected from the surface AQ_E. To describe this we introduce an additional class of rays which include on their trajectory a point Q_R of the surface AQ_E. Applying Fermat's principle, the distance OQ_RP along the ray path is a minimum and the law of reflection results. This simple extension of Fermat's principle which accounts for the reflected ray is so natural that we accept it without question. The field of the reflected ray is readily deduced from image theory as

$$(3) \qquad U^r(P) \equiv U^r(A\text{-}Q_E) = \pm\, C \frac{e^{-jks''}}{\sqrt{s''}} \quad ,$$

where the positive sign is for Neumann (hard) boundary condition associated with the magnetic current line source, the negative sign is for the Dirichlet (soft) boundary condition associated with the electric current source line, and s" is the distance between the image O' and the observation point P. The reflected field vanishes in regions II and III, which the reflected ray does not penetrate. Let us consider now a further extension of Fermat's principle.

B. Singly-Diffracted Rays

It is well known that the ray incident on the edge Q_E in Fig. 2 gives rise to diffraction. To account for this, Keller introduced a class of rays which includes the point Q_E in its trajectory. This completely determines the diffracted ray path in the isotropic, homogeneous medium of this two-dimensional problem, so the law of edge diffraction becomes trivial under these circumstances.

In terms of GTD, the diffracted field at P for the line source at O is

$$(4) \qquad U^d(Q_E) = U^i(Q_E)\, D_{\substack{s\\h}}(\phi,\phi')\, \frac{e^{-jks}}{\sqrt{s}} \quad ,$$

where D_s is the scalar diffraction coefficient for the accoustically soft (Dirichlet) boundary condition and D_h is the scalar diffraction coefficient for the accoustically hard (Neumann) boundary condition. They are deduced from the general dyadic diffraction coefficient $\bar{\bar{D}}(\phi,\phi',\beta_0)$ obtained by Kouyoumjian and Pathak [6,7]. For the special case where the incident ray is perpendicular to a straight edge, the scalar diffraction coefficients are given by

$$(5) \qquad D_{\substack{s\\h}}(\phi,\phi') = \frac{-e^{-j\,\pi/4}}{2n\sqrt{2\pi k}}$$

$$\left\{\left[\cot\left(\frac{\pi+(\phi-\phi')}{2n}\right)F[kLa^+(\phi-\phi')] + \cot\left(\frac{\pi-(\phi-\phi')}{2n}\right)F[kLa^-(\phi-\phi')]\right]\right.$$

$$\left.\pm\left[\cot\left(\frac{\pi+(\phi+\phi')}{2n}\right)F[kLa^+(\phi+\phi')] + \cot\left(\frac{\pi-(\phi+\phi')}{2n}\right)F[kLa^-(\phi+\phi')]\right]\right\}$$

where $n\pi$ is the exterior wedge angle, which equals $3\pi/2$ in this case, and

$$(6) \qquad F(x) = 2j\,|\sqrt{X}|\, e^{jX} \int_{|\sqrt{X}|}^{\infty} e^{-j\tau^2}\, d\tau$$

in which

$$(7) \qquad a^{\pm}(\phi\pm\phi') = 2\cos^2\left(\frac{2n\pi N^{\pm} - (\phi\pm\phi')}{2}\right) .$$

$N^{\pm}$ are the integers which most nearly satisfy the following equations

(8) $$2\pi n N^{+} = \pi + (\phi \pm \phi')$$

(9) $$2\pi n N^{-} = -\pi + (\phi \pm \phi')$$

and kL is the large parameter in the asymptotic evaluation of the pertinent integrals involved in the derivation of the dyadic diffraction coefficient. The quantity L may be viewed as a distance parameter which depends upon the type of edge illumination; for line source illumination, L is given by

(10) $$L = \frac{s\, s'}{s + s'}$$

For grazing incidence $\phi' = 0, n\pi$, D_h is multiplied by a factor of ½; furthermore, if the diffracted ray grazes the surface in the case of a soft boundary, $D_s = 0$ and the diffracted field vanishes, as it should.

The field of the singly-diffracted ray is discontinuous at the shadow and reflection boundaries in a way which compensates the discontinuities in the geometrical optics fields there. This is readily demonstrated; consider for example the incident and diffracted fields at the shadow boundary, where to simplify the discussion, it is assumed there is no nearby reflection boundary. Let $\pi+\phi'-\varepsilon$ be a point close to the shadow boundary, see Fig. 2. In the illuminated region $\varepsilon > 0$ and in the shadow region $\varepsilon < 0$.

(11) $$U(\phi) = \begin{cases} C\,\dfrac{e^{-jks_0}}{\sqrt{s_0}} + C\,\dfrac{e^{-jks'}}{\sqrt{s'}}\, D_{\substack{s\\h}}(\phi'+\pi-\varepsilon,\phi')\,\dfrac{e^{-jks}}{\sqrt{s}}\,, & \varepsilon > 0 \\[2ex] C\,\dfrac{e^{-jks'}}{\sqrt{s'}}\, D_{\substack{s\\h}}(\phi'+\pi-\varepsilon,\phi')\,\dfrac{e^{-jks}}{\sqrt{s}}\,, & \varepsilon < 0 \end{cases}$$

For ε small it follows from Eq. (5) that

(12) $$D_{\substack{s\\h}}(\phi'+\pi-\varepsilon,\phi') = \frac{-e^{-j\,\pi/4}}{2n\sqrt{2\pi k}} \left\{ \cot\frac{\varepsilon}{2n}\; F\left[kLa^{-}(\pi-\varepsilon)\right] \right.$$
$$\left. + \text{ smaller terms which are continuous at the shadow boundary} \right\} .$$

From Eq. (9),

$$N^- = 0$$

Also, as $\varepsilon \to 0$,

(13) $$\cot\left(\frac{\varepsilon}{2n}\right) = \frac{2n}{\varepsilon}$$

(14) $$a^-(\pi-\varepsilon) = \frac{\varepsilon^2}{2}$$

(15) $$F\left[kLa^-(\pi-\varepsilon)\right] = \sqrt{\pi kL/2}\; e^{j\pi/4}\; |\varepsilon|$$

Substituting Eqs. (13) and (15) into Eq. (12) as $\varepsilon \to 0$,

(16) $$D_{\substack{s\\h}}(\phi'+\pi-\varepsilon,\phi') = -\tfrac{1}{2}\sqrt{\frac{s'\,s}{s+s'}}\quad \operatorname{sgn}\varepsilon + \text{smaller, continuous terms,}$$

(17) $$s_0 = s' + s \quad .$$

Upon substituting Eqs. (16) and (17) into Eq. (11), it is seen that the total field is continuous at the shadow boundary. In an analogous manner it can be shown that the total field is continuous at the reflection boundary.

C. Doubly-Diffracted Rays

When one face of the conducting wedge is terminated at Q_F as shown in Fig. 3, a second order diffracted-ray will emanate from the edge Q_F. In terms of the GTD, the doubly-diffracted field at P due to the line source at 0 can be written as

(18) $$U^d(Q_E,Q_F) = U^i(Q_F)\; \tfrac{1}{2}\; D_{\substack{s\\h}}(\phi_2,0)\; \frac{e^{-jks}}{\sqrt{s}}$$

$$= \left\{U^i(Q_E)\; D_{\substack{s\\h}}\left(\frac{3\pi}{2},\phi'\right) \frac{e^{-jkh}}{\sqrt{h}}\right\} \frac{D_{\substack{s\\h}}(\phi_2,0)}{2}\; \frac{e^{-jks}}{\sqrt{s}} \quad .$$

Since $D_s(3\pi/2,\phi') = 0$, the contribution from the doubly-diffracted rays vanishes for the soft boundary according to the above expression. If a higher order approximation for the doubly-diffracted field is employed, then this contribution is non-vanishing, as will be explained later.

The field of the ray singly-diffracted at Q_E has a shadow boundary $SB(Q_E)$ as shown in Fig. 3; the singly-diffracted ray does not penetrate

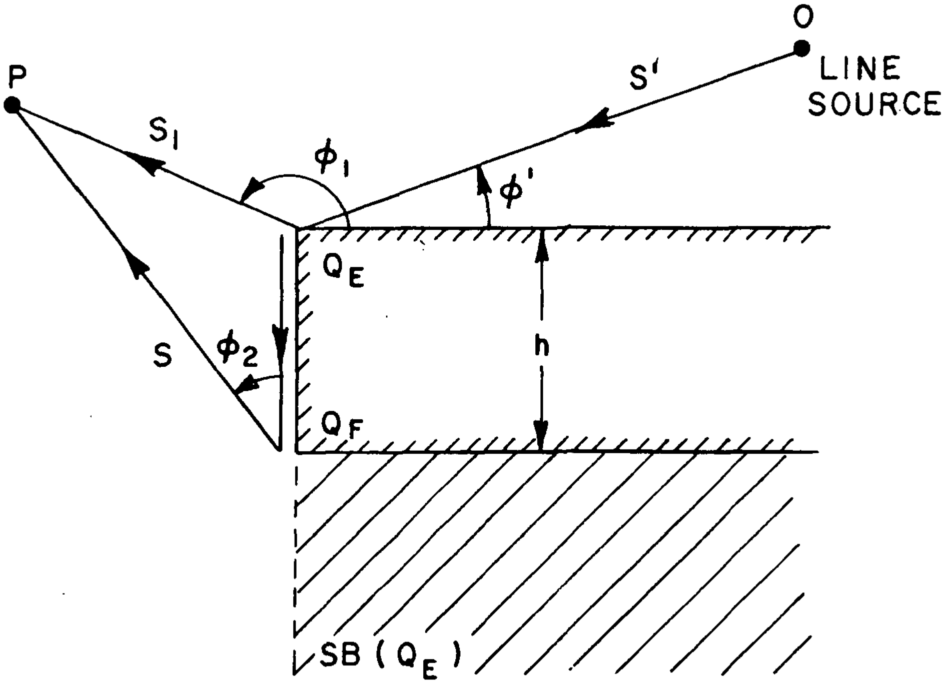

Fig. 3. Configuration for double-diffraction.

the shaded region. It will be shown next that the discontinuity in the field of the singly-diffracted ray at $SB(Q_E)$ is compensated by the ray doubly-diffracted from Q_F, so that the total diffracted field is continuous at this boundary. Since the field doubly diffracted vanishes in the case of the soft boundary, we only need to treat the hard boundary here.

Consider a point close to $SB(Q_E)$ so that $\phi_2 = \pi-\varepsilon$, the total diffracted field at this boundary is

$$(19) \qquad U^{TD} = \begin{cases} U^i(Q_E)\, D_h(\phi_1,\phi')\, \dfrac{e^{-jks_1}}{\sqrt{s_1}} + U^i(Q_F)\dfrac{D_h(\pi-\varepsilon,0)}{2}\,\dfrac{e^{-jks}}{\sqrt{s}}, & \varepsilon > 0 \\ \\ U^i(Q_F)\, \dfrac{D_h(\pi-\varepsilon,0)}{2}\, \dfrac{e^{-jks}}{\sqrt{s}}, & \varepsilon < 0 \end{cases}$$

where s_1, ϕ_1 are the coordinates of the ray diffracted from Q_E, and

(20) $$U^i(Q_F) = U^i(Q_E) D_h\left(\frac{3\pi}{2}, \phi'\right) \frac{e^{-jkh}}{\sqrt{h}} \quad .$$

When $\phi_2' = 0$ and the singly-diffracted ray grazes the vertical surface, the second and fourth terms in the expression for the diffraction coefficient are the same, except for the ± sign of the latter. This is also true for the first and third terms. As a result,

(21) $$D_h(\pi-\varepsilon,0) = \frac{-e^{-j\pi/4}}{n\sqrt{2\pi k}} \left\{ \cot\left(\frac{\varepsilon}{2n}\right) F[kLa^-(\pi-\varepsilon)] \right.$$
$$\left. + \text{ smaller terms which are continuous at } SB(Q_E) \right\} \quad .$$

As $\varepsilon \to 0$, it is seen from Eqs. (12), (13), (14) and (15) that

(22) $$D_h(\pi-\varepsilon,0) = -\sqrt{\frac{hs}{s+h}} \quad \text{sgn } \varepsilon ;$$

furthermore,

(23) $$s_1 = h + s \quad .$$

Substituting Eqs. (22) and (23) into Eq. (19) and making use of Eq. (20), it is seen that the total diffracted field is continuous at the boundary $SB(Q_E)$.

As we have already noted, in the case of a soft boundary the field of an incident-ray grazing the surface vanishes, the edge-diffracted field is then proportional to the normal derivative of the incident field at the edge. The proportionality factor is a diffraction coefficient D' given by Karp and Keller [8]. Thus, for the case of Dirichlet problem, the doubly-diffracted field must be replaced by

(24) $$U^d(Q_E,Q_F) = \frac{\partial U^i(Q_F)}{\partial n} \frac{D'(\phi_2,0)}{2} \frac{e^{-jks}}{\sqrt{s}}$$

where

(25) $$D'(\phi_2,0) = \frac{1}{jk} \frac{\partial}{\partial \phi'} D_s(\phi_2,0)$$

The derivate $\partial U(Q_F)/\partial n$ is taken with respect to the normal to the surface $Q_E Q_F$. This contribution is weak in comparison with that of the singly-diffracted rays; the contribution of the former is of order $(1/k^2)$, whereas that of the latter is of order $(1/\sqrt{k})$. In calculating the field diffracted from the soft cylinder, it was found that the field of the doubly-diffracted rays did not contribute significantly, so the contribution from these rays can be omitted in this case.

Let us now turn to the diffraction by a rectangular cylinder illuminated by a line source. Depending on the location of the line source, the whole domain surrounded by the cylinder will be divided into regions by the various shadow boundaries and the reflection boundaries. Each of these boundaries is labeled to indicate how it originates. For example, referring to Fig. 4, the notation SB means the shadow boundary of the incident geometrical optics field $U^i(P)$, RB(A-B) is the shadow boundary of the geometrical optics field $U^r(A-B)$ reflected from the surface A-B, SB(A) is the shadow boundary of the singly-diffracted $U^d(A)$, which emanates from the edge A, and SB(A,B) is the shadow boundary of the doubly-diffracted field $U^d(A,B)$ which emanates from the edge B. The shadow boundary of the reflected field is referred to simply as the reflection boundary.

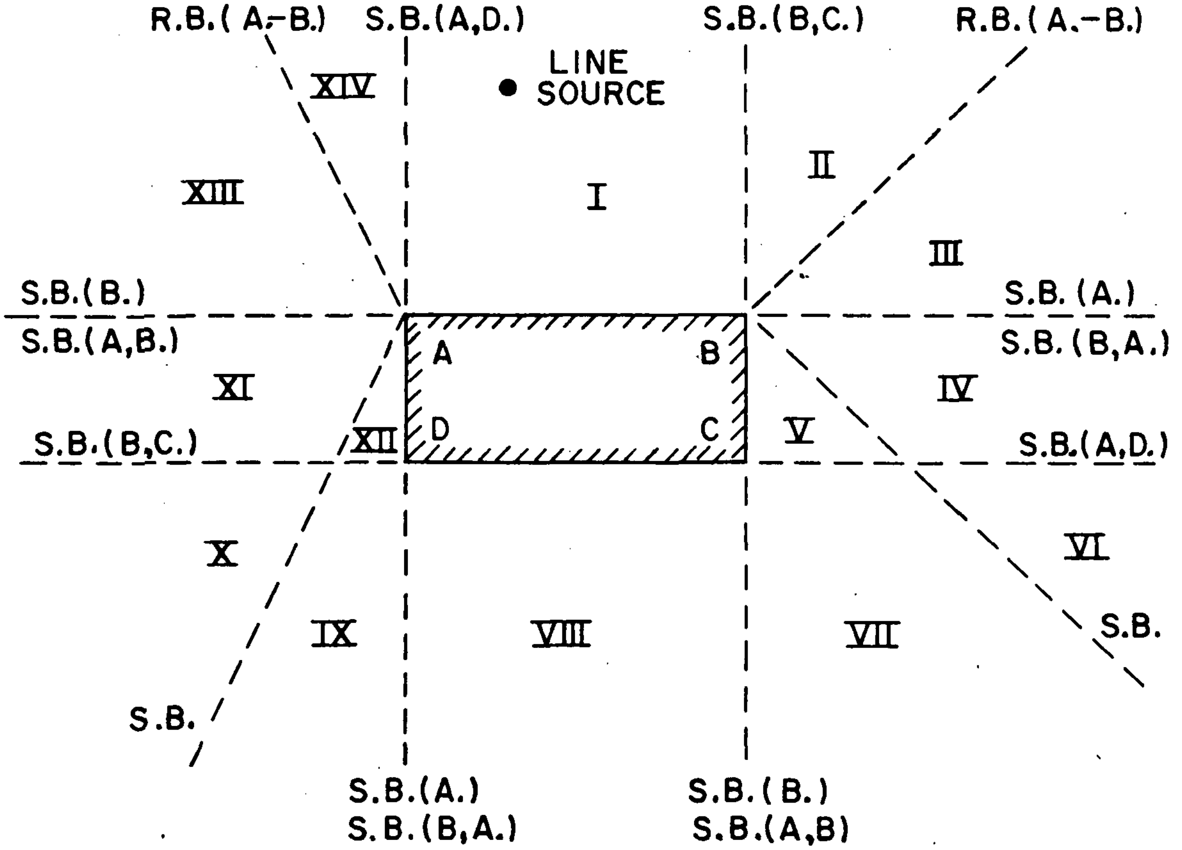

Fig. 4. Shadow and reflection boundaries of the GTD fields.

FIELD \ REGION	I	II	III	IV	V	VI	VII	VIII	IX	X	XI	XII	XIII	XIV
μ^i	✓	✓	✓	✓		✓				✓	✓		✓	✓
$\mu^r(A-B)$	✓	✓												✓
$\mu^d(A)$	✓	✓	✓						✓	✓	✓	✓	✓	✓
$\mu^d(B)$	✓	✓	✓	✓	✓	✓	✓						✓	✓
$\mu^d(A,B)$	✓	✓	✓	✓	✓	✓	✓						✓	✓
$\mu^d(B,A)$	✓	✓	✓						✓	✓	✓	✓	✓	✓
$\mu^d(A,D)$						✓	✓	✓	✓	✓	✓	✓	✓	✓
$\mu^d(B,C)$		✓	✓	✓	✓	✓	✓	✓	✓	✓				

A CHECK (✓) MEANS THE FIELD IS NON-VANISHING IN THE REGION

TABLE I

In what follows we may locate the line source in the upper left hand quadrant of the space surrounding the cylinder, without loss of generality. Three cases will be considered.

1) First, the line source is located directly above the cylinder. The whole domain around the cylinder is divided into 14 regions as shown in Fig. 4. Table I shows the regions covered by each type of ray. To demonstrate the use of the table, let us consider an observation point P in region IX. Examining the column under region IX of Table I, one finds checks(✓) for $U^d(A)$, $U^d(B,A)$, $U^d(A,D)$, and $U^d(B,C)$. Thus the total field at P is equal to $U^T(P) = U^d(A) + U^d(B,A) + U^d(A,D) + U^d(B,C)$.

2) The line source is located to the upper left of the cylinder as shown in Fig. 5. In this case there are 18 regions. Table II shows the regions where a particular ray exists and its field makes a non-vanishing contribution.

3) Line source at grazing incidence. Let the line source be located in the plane which contains the A-D side of the rectangular cylinder as shown in Fig. 6. This case is of special interest because the trailing edge D lies in the shadow of the leading edge A. Also, it lies on the shadow boundary of the direct geometrical optics field. The behavior of the field at the boundary DP must be treated separately, see Appendix I. As before, the domain surrounding the cylinder is divided into regions as shown in Fig. 6 and Table III gives the regions covered by the individual rays.

Recall that one or more of the various field components is discontinuous at each boundary shown in Figs. 4, 5 and 6 but that all except the discontinuities in the doubly diffracted fields are compensated; e.g., the discontinuities in the geometrical optics field are compensated by the field of the singly-diffracted rays and the discontinuities in the field of the singly-diffracted rays are compensated by the fields of the doubly-diffracted rays.

As a final step in the anslysis, the fields of the individual line sources are superimposed to give the field of a linear array of line sources radiating in the presence of the cylinder, see Fig. 7. A computer program has been written to calculate the incident, total and scattered fields once the linear array is specified. Unlike its earlier definition for geometrical optics, the term incident field used here means the field of the array in the absence of the cylinder, and the scattered field is simply the difference between the total field and this incident field. The versatility of such a program is evident; the scattering from the cylinder for a wide variety of illuminations can be studied, and the radiation from antennas in the presence of the rectangular cylinder also can be studied. As a matter of fact, the program was written originally so that the linear array of line sources, when densely packed, closely approximates the field of an aperture antenna of finite width W. The aperture antenna (more precisely its axis) is directed toward a point Q on the surface of the rectangular cylinder as shown in Fig. 7. A description of the aperture radiation in terms of an array of discrete line sources is discussed in the following paragraphs.

The aperture distribution may be approximated by a discrete array of line sources which are properly weighted in amplitude and phase. The width of the aperture denoted by W, is divided into 2M segments; (M = integer). The line sources are positioned at the ends of these segments, which introduces 2M + 1 line sources. In approximating a continuous distribution, the number M is selected so that $2M + 1 \geq 10\ W/\lambda$, where λ = free space radiated wavelength.

Three types of line sources are available in this program:

Type I	An electric current line source
Type II	A magnetic current line source
Type III	A magnetic current moment line source.

As described earlier, the electric current line source radiates an omnidirectional electric field which is parallel to the edge of the rectangular cylinder, and the magnetic current line source radiates an omnidirectional magnetic field which is parallel to the edge of the rectangular cylinder. The magnetic current moment line source consists of a continuous array of magnetic current moments directed perpendicular to the line of the array and parallel to the aperture in question. This line source radiates an electric field parallel to the edge of the cylinder; however, the field has a pattern, $|\cos\theta|$, where θ is shown in Fig. 7. The strength of these magnetic type line sources is determined from the equivalent magnetic surface currents in the aperture. $\overline{K_S} = \overline{E} \times \hat{n}$, where $\overline{E}$ is the electric field distribution in the aperture (assumed known) and $\hat{n}$ is the outward normal to the aperture.

The field of the two-dimensional aperture can be adequately represented in the forward direction by a densely-packed array of type II and type III line sources, but such an array fails to approximate the field adequately at aspects behind the aperture. This limitation is particularly troublesome when calculating the total field. To overcome this difficulty an obliquity factor has been included in the program which multiplies the pattern of each line source. The obliquity factor is $f(\theta) = \cos^n \theta/2$, where $n = 0, \frac{1}{2}, 1, 2$. When $n = 0$, the obliquity factor is unity so that the array radiates symmetrically with respect to the axis of its elements. The case $n = 2$ occurs naturally in the description of the radiation fields of aperture antennas via the Kirchhoff-Huygen's approximation (for the forward region). The cases $n = \frac{1}{2}$, and $n = 1$ are added so that the n which best approximates the measured aperture pattern may be used. It is evident that the obliquity factor results in a pattern null in the direction directly behind the aperture at $\theta = \pi$. In most practical cases, there is no such null in the backward direction.

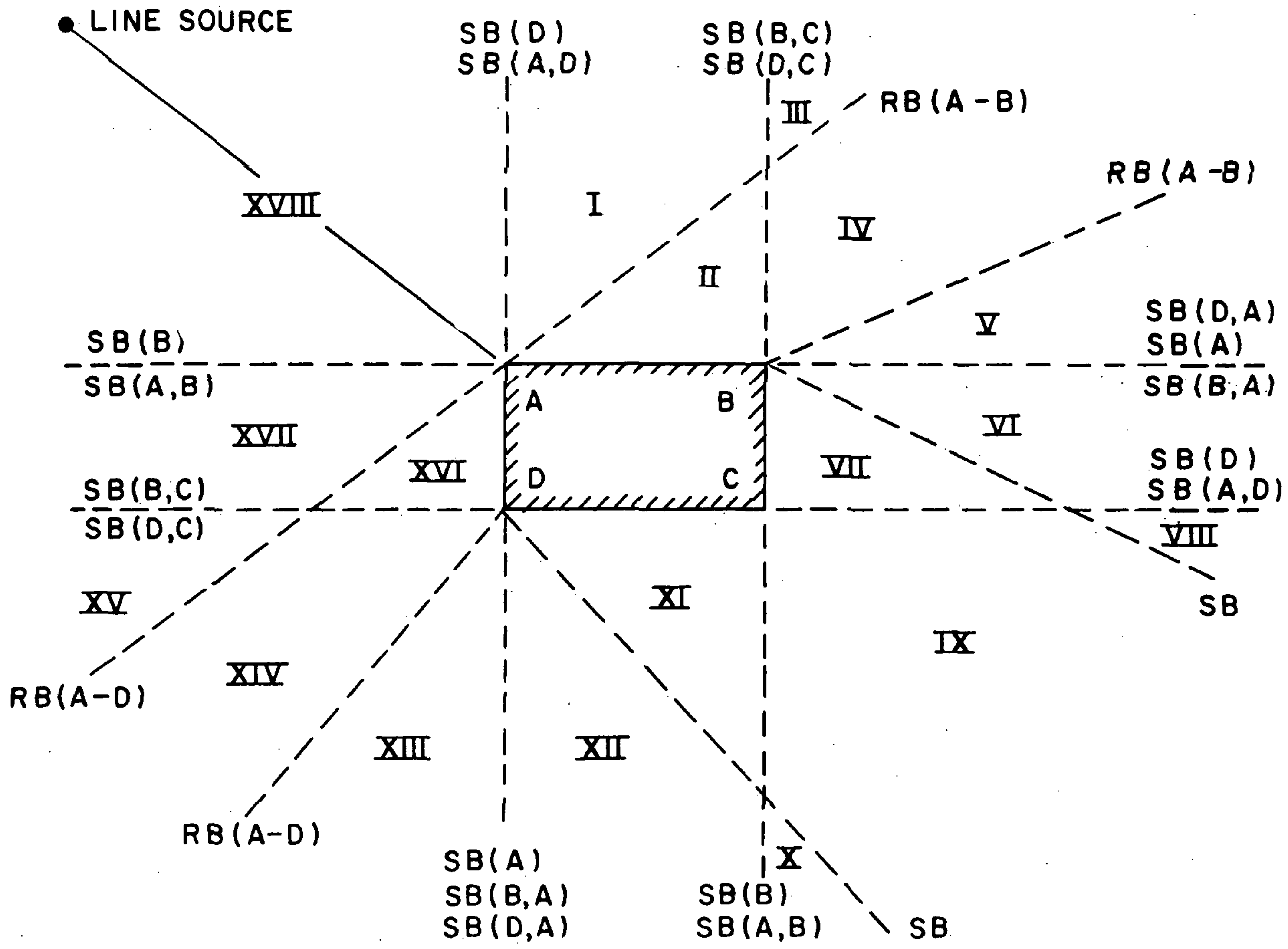

Fig. 5. Shadow and reflection boundaries of the GTD fields

REGION / FIELD	I	II	III	IV	V	VI	VII	VIII	IX	X	XI	XII	XIII	XIV	XV	XVI	XVII	XVIII
μ^{i}	✓	✓	✓	✓	✓	✓		✓		✓		✓	✓	✓	✓	✓	✓	✓
$\mu^{r}(A-B)$		✓		✓														
$\mu^{r}(A-D)$														✓		✓		
$\mu^{d}(A)$	✓	✓	✓	✓	✓								✓	✓	✓	✓	✓	✓
$\mu^{d}(B)$	✓	✓	✓	✓	✓	✓	✓	✓	✓	✓								✓
$\mu^{d}(D)$								✓	✓	✓	✓	✓	✓	✓	✓	✓	✓	✓
$\mu^{d}(A,B)$	✓	✓	✓	✓	✓	✓	✓	✓	✓	✓								✓
$\mu^{d}(B,A)$	✓	✓	✓	✓	✓								✓	✓	✓	✓	✓	✓
$\mu^{d}(A,D)$								✓	✓	✓	✓	✓	✓	✓	✓	✓	✓	✓
$\mu^{d}(D,A)$	✓	✓	✓	✓	✓								✓	✓	✓	✓	✓	✓
$\mu^{d}(B,C)$			✓	✓	✓	✓	✓	✓	✓	✓	✓	✓	✓	✓	✓			
$\mu^{d}(D,C)$			✓	✓	✓	✓	✓	✓	✓	✓	✓	✓	✓	✓	✓			

TABLE II

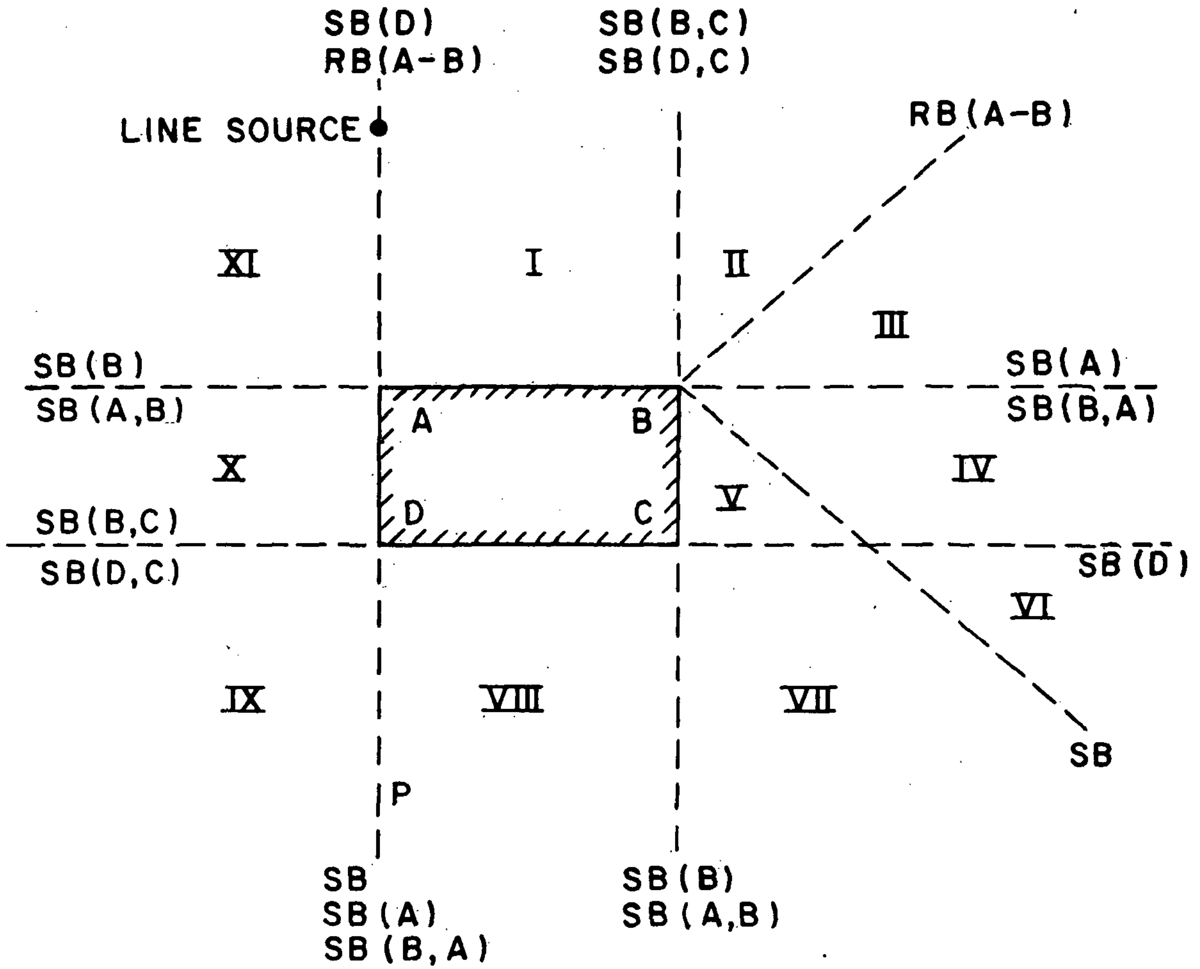

Fig. 6. Shadow and reflection boundaries of the GTD fields.

REGION / FIELD	I	II	III	IV	V	VI	VII	VIII	IX	X	XI
μ^i (p)	✓	✓	✓	✓		✓			✓	✓	✓
μ^r (A–B)	✓	✓									
μ^d (A)	✓	✓	✓						✓	✓	✓
μ^d (B)	✓	✓	✓	✓	✓	✓	✓				✓
* μ^d (D)						✓	✓	✓	✓	✓	✓
μ^d (A,B)	✓	✓	✓	✓	✓	✓	✓				✓
μ^d (B,A)	✓	✓	✓						✓	✓	✓
μ^d (B,C)		✓	✓	✓	✓	✓	✓	✓	✓		
μ^d (D,C)		✓	✓	✓	✓	✓	✓	✓	✓		

* SEE APPENDIX I

TABLE III

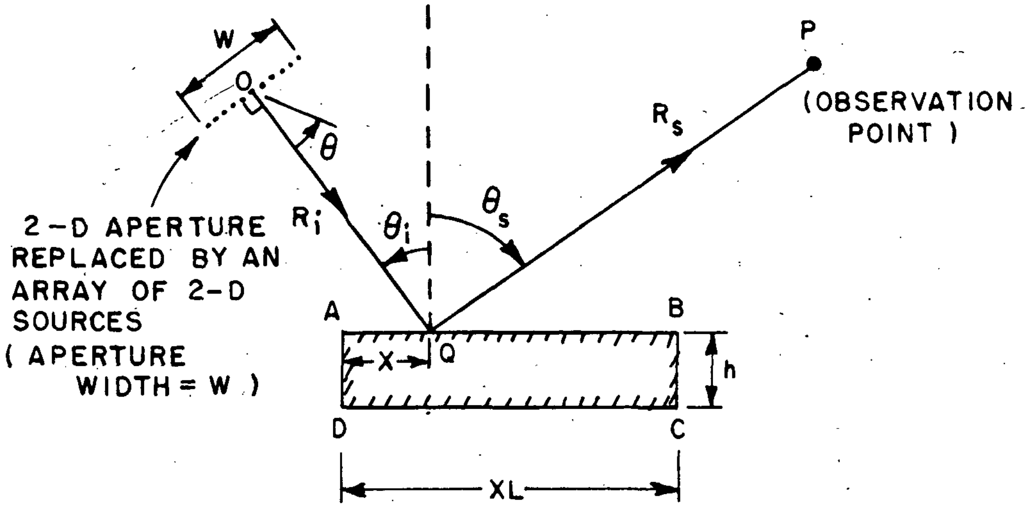

Fig. 7. An array of line source in the presence of the rectangular cylinder.

On the other hand, the pattern in the forward region is quite satisfactory when the obliquity factor is included, and as one moves away from the forward region, the pattern drops to a level where the differences between the simulated and measured patterns are unimportant when computing the total field surrounding the rectangular cylinder.

The scattered, and the total fields are computed as a function of $\theta_s(-\pi \leq \theta_s \leq \pi)$ at a range R_s. The incident field pattern on the other hand is available for a phase reference at the center of the array (aperture) at O in Fig. 7 and computed at a range measured from O, as well as for a phase reference at Q with a range R_s (just as for the scattered and the total fields).

The input and output variables for the computer program are described in Appendix II, and the listing of the computer program is given. Also, a sample case is treated in this appendix to illustrate the use of the program.

III. NUMERICAL RESULTS

To assess the accuracy of the GTD solution described in the preceding section, it was applied to several simple examples, where the rectangular cylinder is illuminated by either an electric or magnetic current line source. Far-zone patterns for the total field are calculated by this method and also from numerical solutions of the pertinent integral equation*. The cylinders are square with a side length of 1.6

*The computer programs for the integral equation solutions were provided by Prof. J.H. Richmond of the ElectroScience Laboratory.

wavelength, and in each case the line source illuminates the cylinder from a distance of 0.8 wavelength. These small distances provide a stringent test of our GTD solution; also they give us an opportunity to examine the accuracy of the new scalar diffraction coefficients in a situation where the edges are illuminated by curved wavefronts and where the transition regions are relatively broad. The pattern calculated from the integral equation solution must be considered more accurate for the small dimensions chosen for these examples, since the integral equation method is convergent whereas the GTD solution is an asymptotic approximation.

Patterns for magnetic current line source excitation (hard boundary case) are given in Figs. 8, 9 and 10, where the line source is positioned on the diagonal of the square cylinder, on the centerline directly above the cylinder, and at a point of glancing incidence on one of its surfaces. The agreement between the patterns calculated by the GTD and the integral equation method is remarkable - every detail is the same within the limits of graphical accuracy. The corresponding patterns for electric current line source excitation (soft boundary case) are presented in Figs. 11, 12 and 13. Again there is excellent agreement between the two pattern calculations, except in the vicinity region of forward scatter in Figs. 12 and 13. Note that the level of the patterns is very low in these regions, so that small errors in the solution become significant. We hope to look into the reason for these differences at a later time.

The numerical examples considered here confirm the accuracy and applicability of our GTD solution; this is further demonstrated by an example treated in Appendix II. As the size of the cylinder and the distance between the edges of the cylinder and the source (or sources) increases in terms of a wavelength, one can expect the accuracy of the GTD solution to increase, because it is an asymptotic approximation where $k = 2\pi/\lambda$ is a large parameter.

In the case of magnetic current line source excitation there is little evidence of shadowing in the forward direction by the small square cylinder; however, there is distinct evidence of shadowing in the case of electric current line source excitation, where the total electric field is parallel to the cylinder and must vanish at its surface. One should expect this.

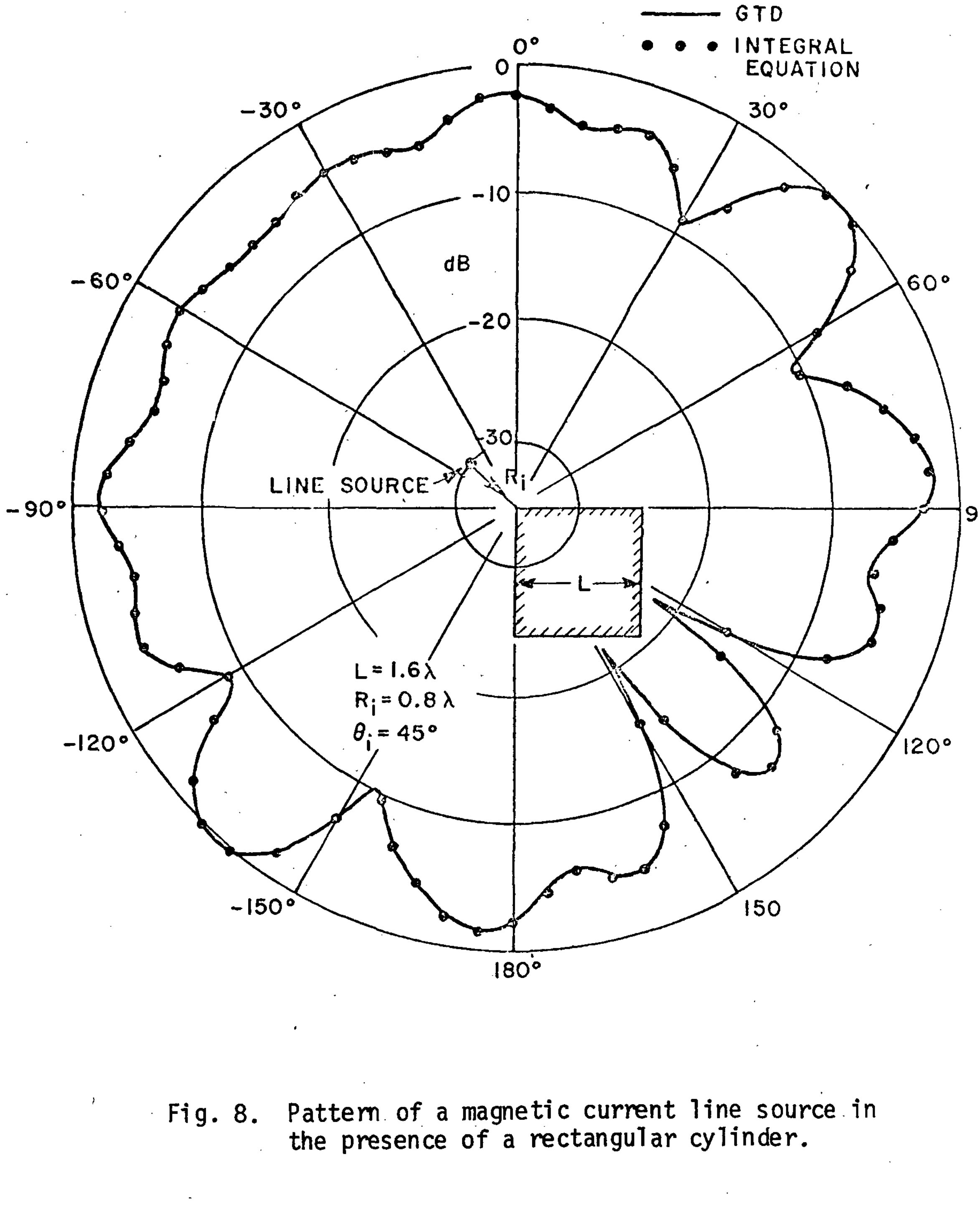

Fig. 8. Pattern of a magnetic current line source in the presence of a rectangular cylinder.

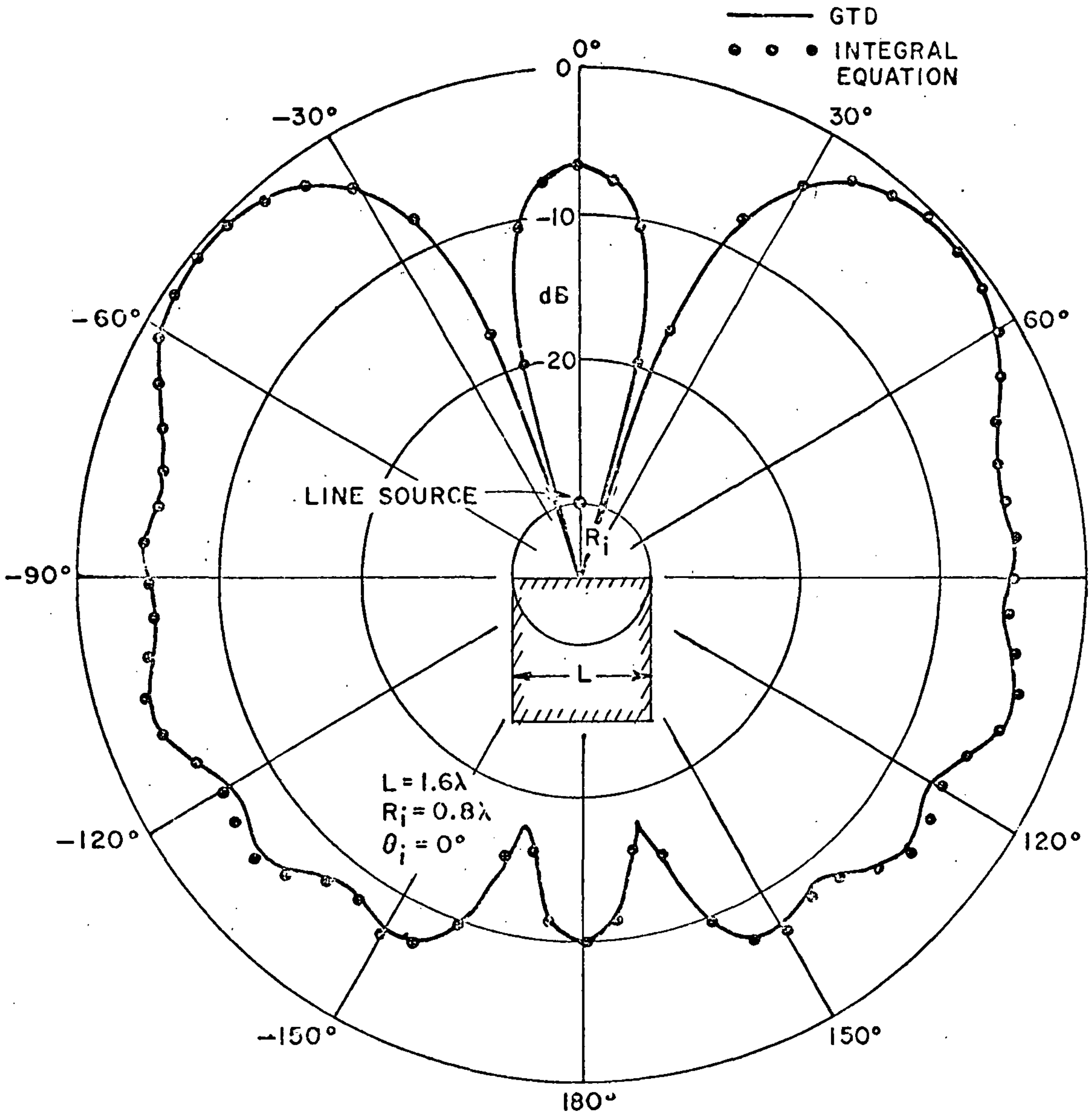

Fig. 9. Pattern of a magnetic current line source in the presence of a rectangular cylinder.

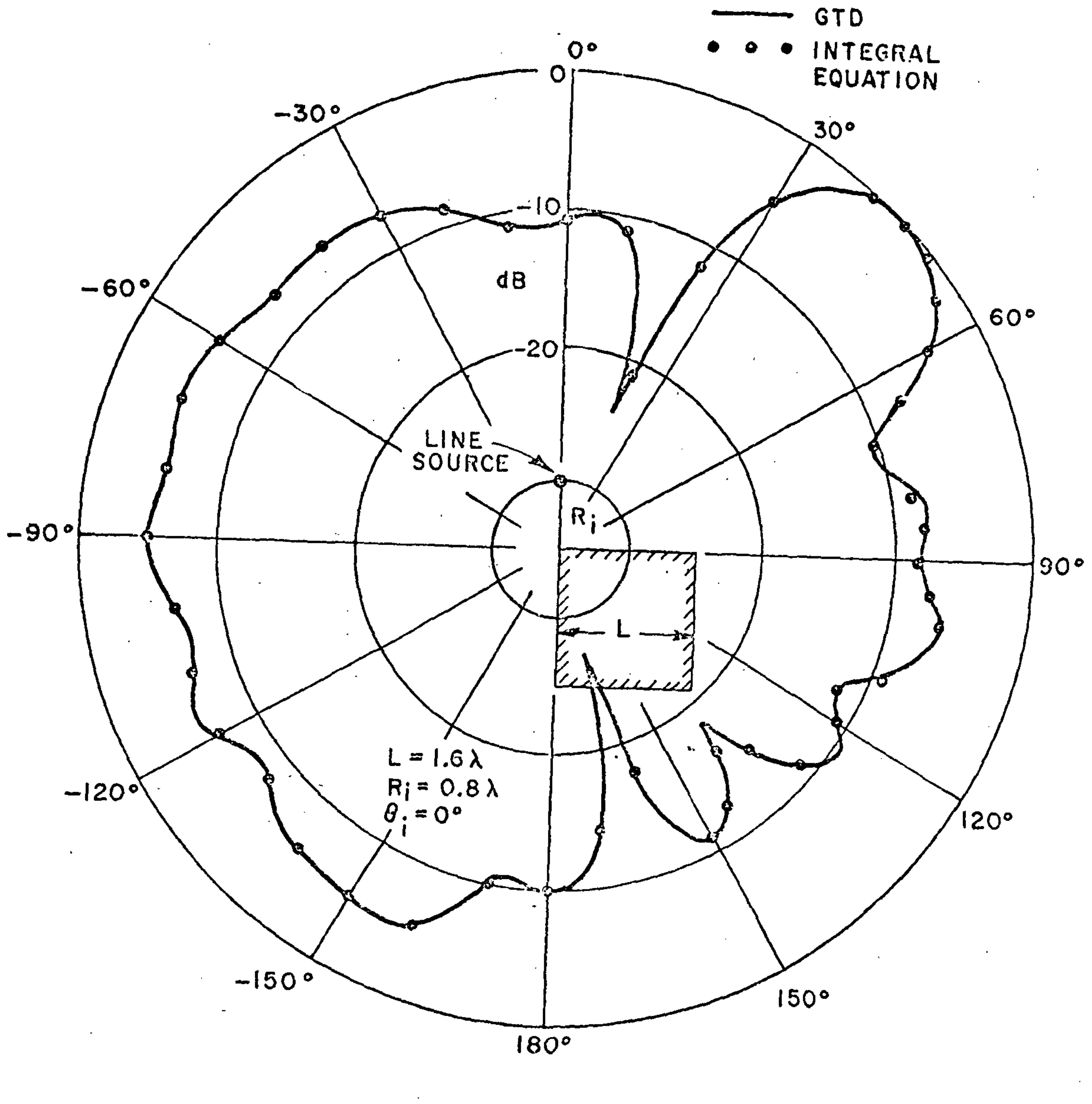

Fig. 10. Pattern of a magnetic current line source in the presence of a rectangular cylinder.

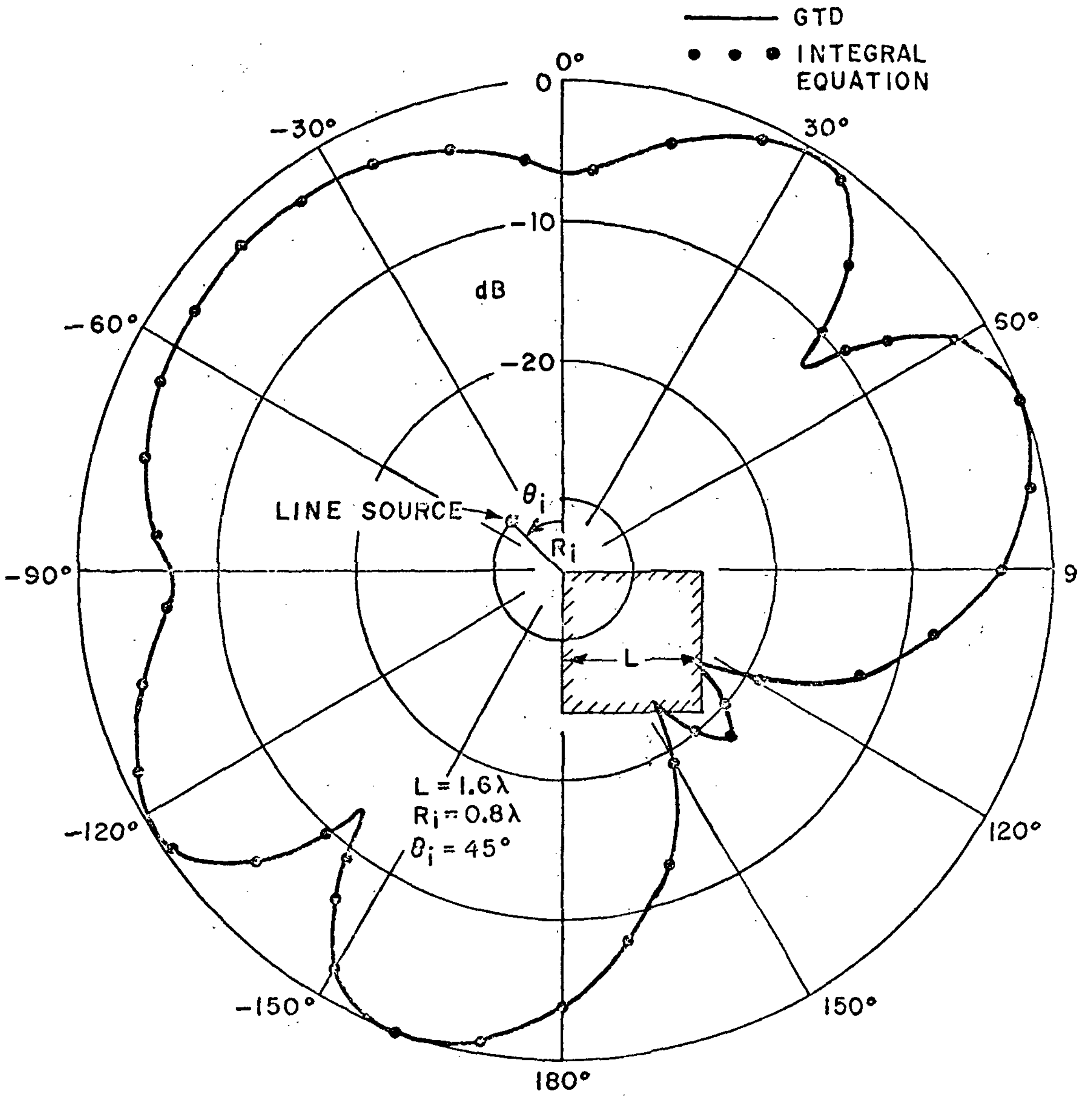

Fig. 11. Pattern of an electric current line source in the presence of a rectangular cylinder.

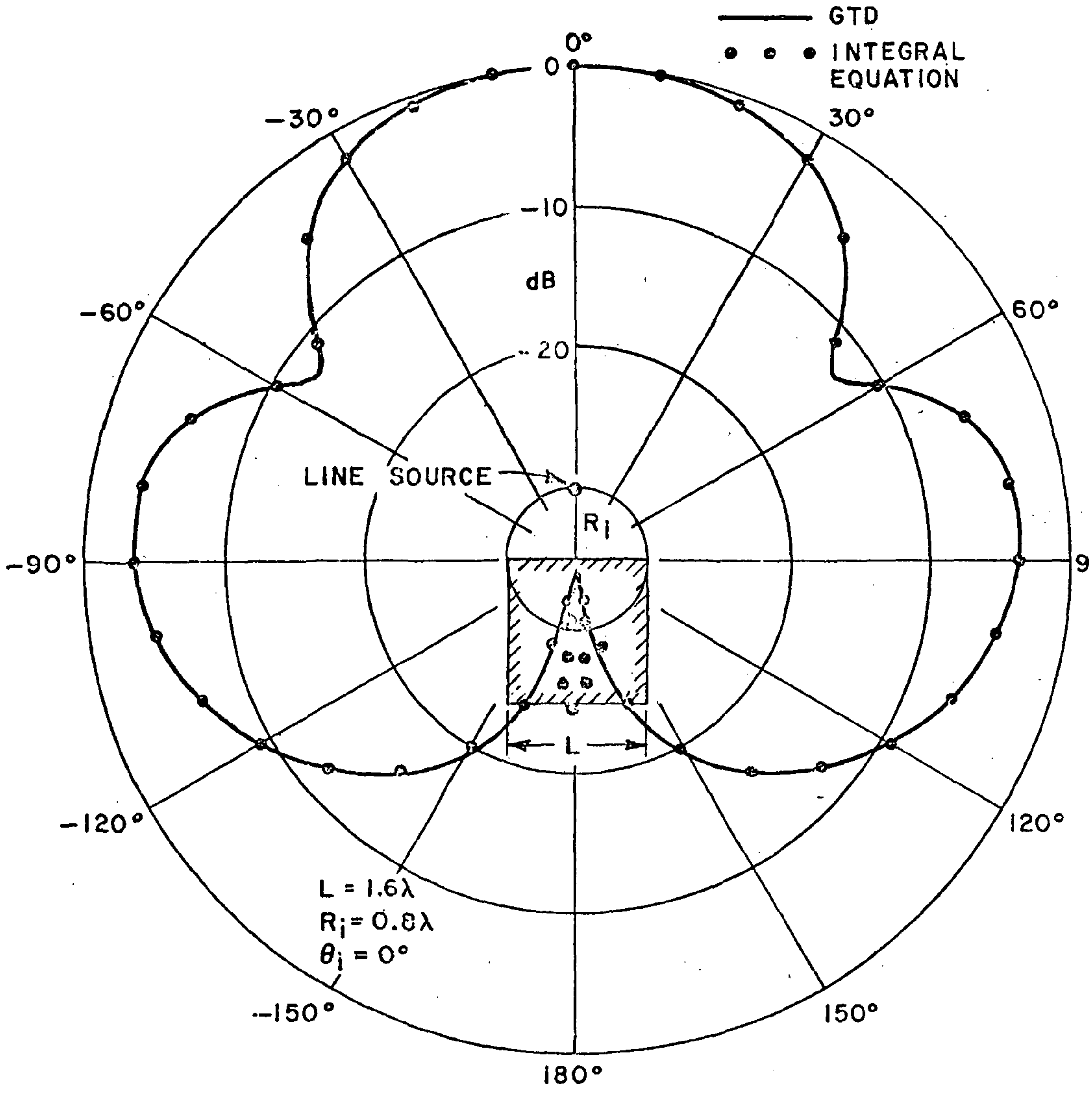

Fig. 12. Pattern of an electric current line source in the presence of a rectangular cylinder.

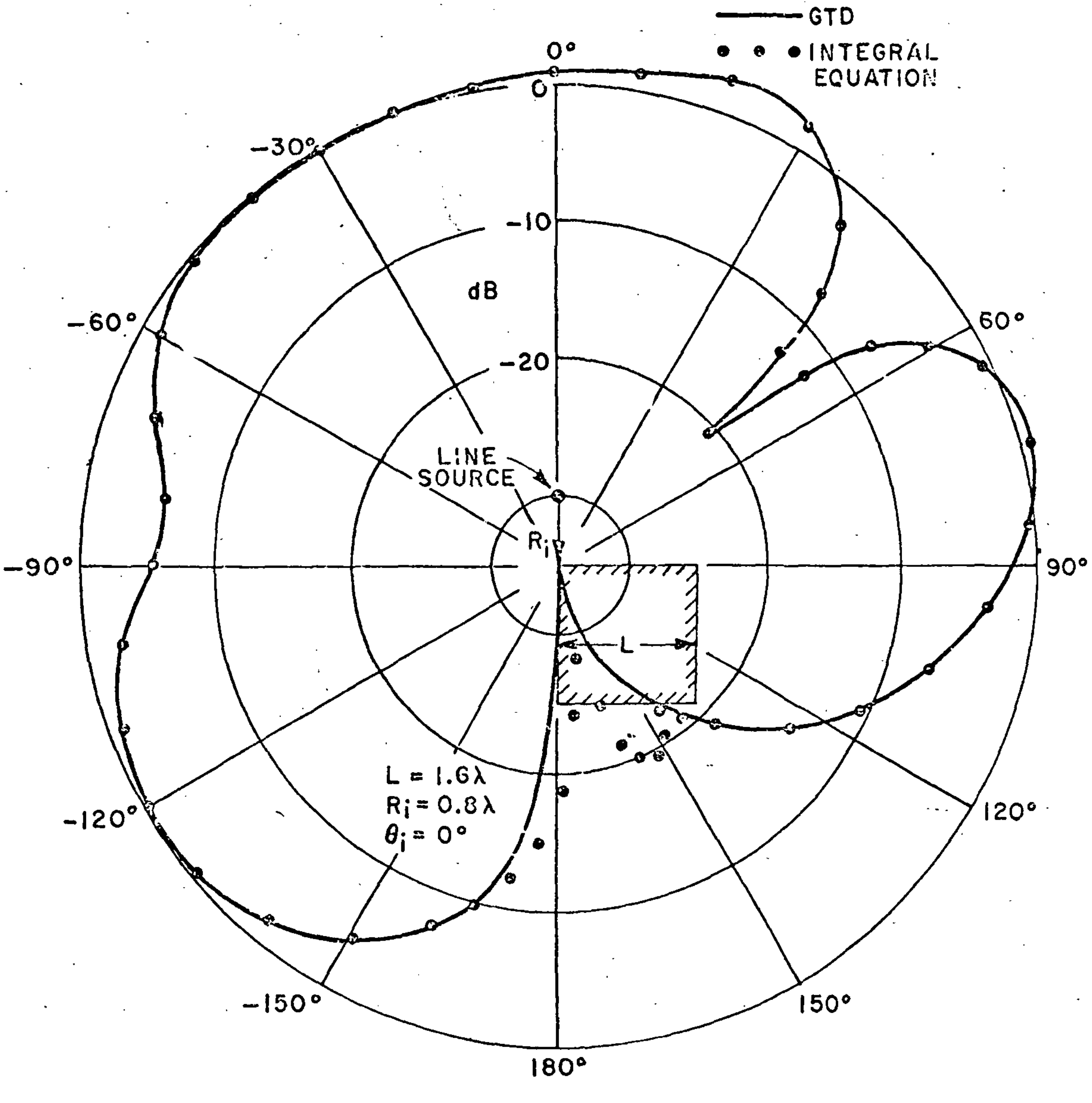

Fig. 13. Pattern of an electric current line source in the presence of a rectangular cylinder.

IV. CONCLUSIONS

The GTD has been applied to calculate the radiation from a perfectly-conducting rectangular cylinder in the presence of a linear array of line sources, which may be of the electric current, magnetic current or magnetic current moment type. When densely packed, these sources may be used to approximate the radiation from an aperture. To insure good accuracy in the fields calculated from the solution described here, the separation of source and field points from the edges of the cylinder and the separation of the edges from each other should be not less than 0.7 wavelength. However, for far-zone pattern calculations, the line sources can be only a few tenth of a wavelength from the nearest edge.

The use of new scalar diffraction coefficients valid in the transition regions makes it possible to calculate continuous patterns in the region surrounding the cylinder away from its edges. Radiation patterns calculated from this solution and from an integral equation solution are found to be in excellent agreement for a number of stringent test cases. This demonstrates the utility and accuracy of the new diffraction coefficients and the overall accuracy of GTD as it has been applied to this problem.

APPENDIX I

THE FIELD AT THE SHADOW BOUNDARY OF A THICK SCREEN FOR GRAZING INCIDENCE

In this appendix we derive an expression for the field near the shadow boundary of a thick, perfectly conducting screen illuminated by a line source at grazing incidence, as shown in Fig. 14. The solution near the shadow boundary in the forward direction is of interest. In the following development we employ Eqs. (5) through (10) in the text, the subscript h on the hard scalar diffraction coefficient has been omitted, and it is convenient to use the function

$$f(x) = \frac{e^{-jkx}}{\sqrt{x}} \qquad \text{(A-1)}$$

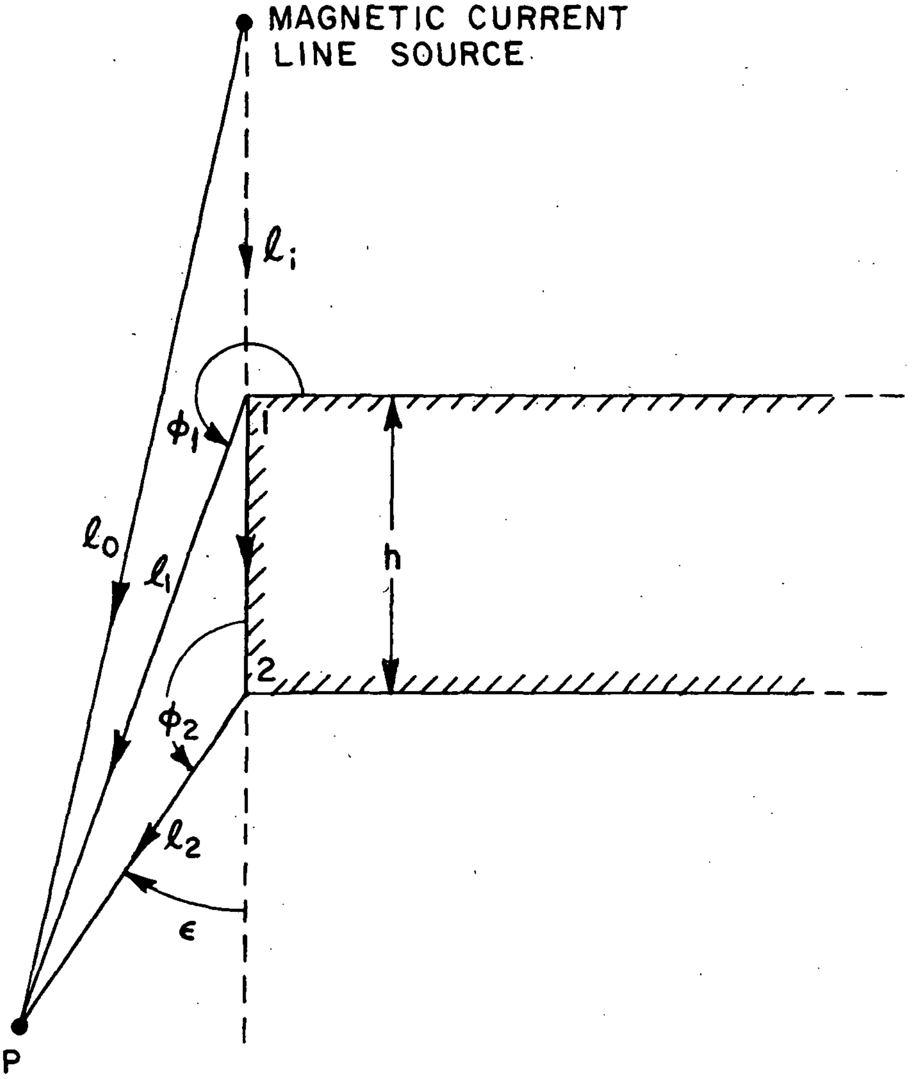

Fig. 14. Shadow boundary of a thick screen for grazing incidence.

Let the strength of the line source be such that the incident field at P is

$$U^i(P) = f(\ell_0) \quad . \tag{A-2}$$

The total field at P is the sum of the incident field plus the field of the ray singly-diffracted from edge 1 and the field of the ray doubly-diffracted from edge 2. In the illuminated region, $\varepsilon > 0$,

$$U(P) = f(\ell_0) + f(\ell_i)\ D(\phi_1,\tfrac{\pi}{2};L_1)\ f(\ell_1) + \tfrac{1}{2}U^i(2)\ D(\phi_2,0,L)\ f(\ell_2) \quad . \tag{A-3a}$$

In the shadow region, $\varepsilon < 0$,

$$U(P) = \tfrac{1}{2}U^i(2)\ D(\phi_2,0,L)\ f(\ell_2) \quad . \tag{A-3b}$$

Here,

$$\phi_2 = \pi - \varepsilon \quad , \tag{A-4a}$$

$$L_1 = \frac{\ell_i\ \ell_1}{\ell_i + \ell_1} \quad , \tag{A-4b}$$

$$U^i(2) = f(\ell_i+h) + f(\ell_i)\left[-\frac{2}{3}e^{-j\pi/4}\cot(\frac{2\pi}{3})\ F(2kL_1')\right]f(h) \tag{A-4c}$$

in which

$$L_1' = \frac{\ell_i\ h}{\ell_i + h} \quad . \tag{A-4d}$$

Thus for $\varepsilon > 0$,

$$\begin{aligned} U(P) = {} & f(\ell_0) + f(\ell_i)\ D(\phi_1,0;L_1)\ f(\ell_1) + \tfrac{1}{2}f(\ell_i+h)\ D(\phi_2,0;L_2)f(\ell_2) \\ & + \tfrac{1}{2}f(\ell_i)f(h)\ \left[-\frac{2}{3}e^{-j\pi/4}\cot(\frac{2\pi}{3})\ F(2kL_1')\right]\ D(\phi_2,0,\overline{L})\ f(\ell_2) \quad , \end{aligned} \tag{A-5a}$$

and for $\varepsilon < 0$,

$$\text{(A-5b)} \qquad U(P) = \tfrac{1}{2} f(\ell_i + h)\, D(\phi_2, 0, L_2)\, f(\ell_2) + \tfrac{1}{2} f(\ell_i) f(h) \cdot \left[-\frac{2}{3} e^{-j\pi/4} \cot\left(\frac{2\pi}{3}\right) F(2kL_1')\right] D(\phi_2, 0, \bar{L})\, f(\ell_2) \quad ,$$

where

$$\text{(A-6)} \qquad L_2 = \frac{(\ell_i + h)\,\ell_2}{\ell_i + h + \ell_2}$$

and $\bar{L}$ is a distance parameter determined by the wavefront curvature of the field incident on edge 2 which has been singly-diffracted from edge 1. Since edge 2 is in the transition region of this field, the curvature of this wavefront is not simply that of a cylindrical wave emanating from edge 1; i.e., $\bar{L} \neq h\,\ell_2/(h+\ell_2)$. We will determine $\bar{L}$ by requiring U(P) to be continuous at the shadow boundary.

As $\varepsilon \to 0$,

$$\text{(A-7)} \qquad D(\phi_2, 0, L_2) = \frac{-e^{-j\pi/4}}{n\sqrt{2\pi k}} \left(\frac{2n}{\varepsilon}\right) \sqrt{\frac{\pi k L_2}{2}}\, |\varepsilon|\, e^{j\pi/4}$$

$$= -\sqrt{L_2}\ \mathrm{sgn}\ \varepsilon \quad .$$

In a similar manner,

$$\text{(A-8)} \qquad D(\phi_2, 0, \bar{L}) = -\sqrt{\bar{L}}\ \mathrm{sgn}\ \varepsilon \quad .$$

Furthermore, as $\varepsilon \to 0$

$$\text{(A-9)} \qquad D(\phi_1, 0; L_1) = -\frac{2}{3} e^{-j\pi/4} \cot\left(\frac{2\pi}{3}\right) \frac{F(2kL_1)}{\sqrt{2\pi k}}$$

Substituting Eqs. (A-7), (A-8) and (A-9) into Eqs. (A-5a), (A-5b) and requiring U(P) to be continuous at the shadow boundary $\varepsilon = 0$, we see that

$$(A\text{-}10)\qquad \frac{e^{jk(\ell_i+\ell_1)}}{\sqrt{\ell_i\ \ell_1}}\left\{-\frac{2}{3}e^{-j\ \pi/4}\cot\left(\frac{2\pi}{3}\right)\frac{F(2kL_1)}{\sqrt{2\pi k}}\right\} =$$

$$\frac{e^{-jk(\ell_i+h+\ell_2)}}{\sqrt{\ell_i\ h\ \ell_2}}\left\{-\frac{2}{3}e^{-j\ \pi/4}\cot\left(\frac{2\pi}{3}\right)\frac{F(2kL_1')}{\sqrt{2\pi k}}\right\}\sqrt{\overline{L}}$$

where $h + \ell_2 = \ell_1$ at $\varepsilon = 0$.

From which

$$(A\text{-}11)\qquad \overline{L} = \left(\frac{h\ \ell_2}{h + \ell_2}\right)m$$

with

$$(A\text{-}12)\qquad m = \left[\frac{F(2kL_1)}{F(2kL_1')}\right]^2$$

APPENDIX II

DESCRIPTION OF THE COMPUTER PROGRAM

A. Input Variables

N : is the number of sources in the array which approximates the aperture distribution. Here N = 2M+1, where M is an integer (.. N is an odd integer), and M has been introduced earlier in section II. The DIMENSION cards at the beginning of the program must be dimensioned as N or larger.

TYPE : is a reference parameter. TYPE is set equal to 1.0 when sources of type I (see section II) are used. TYPE is likewise set equal to 2.0 for type II, and is set equal to 3.0 for type III sources, respectively.

AL : is the aperture width (= W of Fig. 7).

AM(I): is the magnitude of the Ith source in the array which approximates a given aperture distribution.

AP(I): is the phase of the Ith line source in the array (which approximates a given aperture distribution), in RADIANS.

X : is the point of incidence on the 2-D box and corresponds to X shown in Fig. 7.

XL : is the length of the box (corresponding to XL of Fig. 7).

H : is the height of the box (it corresponds to h in Fig. 7).

RI : is the incident range (corresponding to R_i in Fig. 7).

RS : is the scattered range (corresponding to R_s in Fig. 7).

THI : is the angle of incidence (corresponding to θ_i in Fig. 7).

XLAMDA: is the transmitted wavelength.

Note that the variables AL, XL, H, X, RI and RS have the same units as XLAMDA.

B. Output Variables

THS : is the angle of scattering (corresponding to θ_s in Fig. 7) in degrees.

ATAL : magnitude of the total field.

DBTAL: magnitude of the total field in dB.

DBSAS: magnitude of the scattered field in dB.

DBGA : incident field with phase center at Q (Fig. 7) as a function of THS, in dB.

PHASE: phase of the total field in degrees.

TH : angular variable corresponding to (Fig. 7), in degrees

DBHA : incident field with phase center at O (Fig. 7) in dB, as a function of TH. Note that DBHA is an output variable in the Subroutine TEST.

C. Instructions for Representing Aperture Field Distribution by a 2-D Line Source Array.

When dealing with the input variables AM(I) and AP(I) for Ith source in the planar array used to approximate a given aperture distribution, the ordering of the array elements is done as follows:

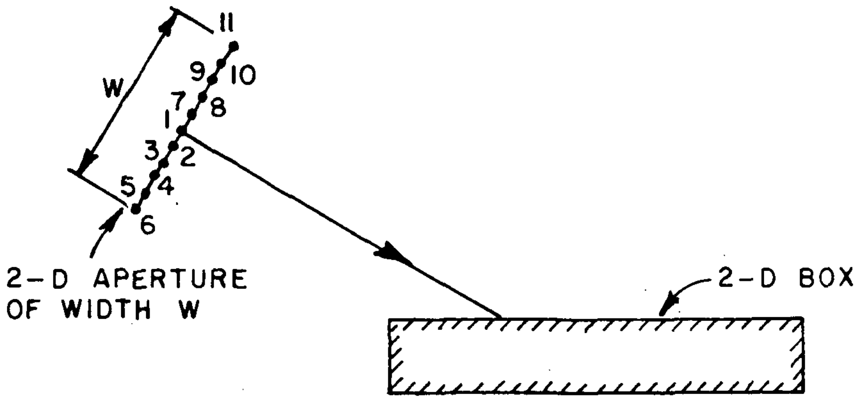

Fig. 15. The ordering arrangement of the line sources used to approximate a given aperture distribution.

Let N = 11, where N is the number of line sources approximating a given aperture distribution over the aperture width W. The ordering arrangement for these sources is indicated in Fig. 15. The source at the center of the aperture is the one for which I = 1. I = 2,3,4,5 and 6 for sources to the right of the one designated by I = 1 (as one views the 2-D box from the aperture center). Similarly, I = 7,8,9,10 and 11 for sources to the left of the source at the center (designated by I = 1).

Let the aperture distribution (assumed known) be represented by the quantity $F = |F|e^{i\psi}$ over the aperture. $|F|$ represents the magnitude of the field distribution over the width W, and ψ represents the phase of the field distribution over the width W. Hypothetical plots of $|F|$ and ψ over the aperture are indicated below:

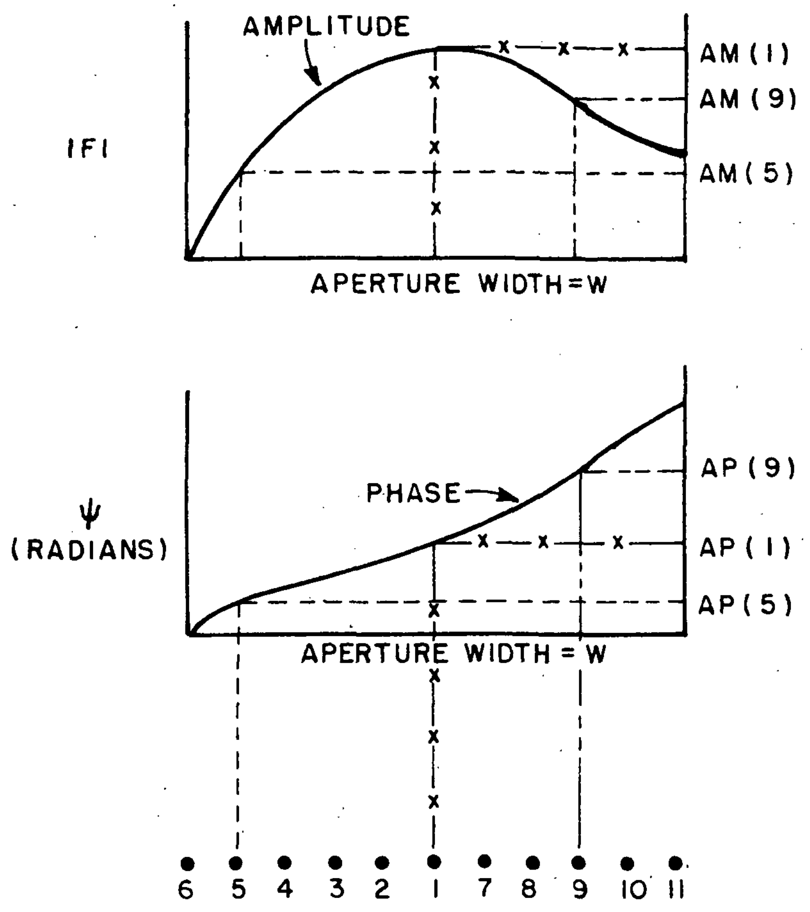

Fig. 16. Field distribution over the aperture.

Fig. 16 clearly indicates the amplitudes and phases of the sources designated by I = 1, 5 and 9. For example, the magnitude of the line source strength corresponding to I = 9 is given by AM(9), and its phase is given by AP(9). Similarly, one can obtain the amplitudes and phases of all the other line sources. Note that the aperture is divided into 2M segments, where M = 5. Hence, the number of sources, N = 2M+1 = 11.

D. Instructions for Using the 'Obliquity Factor'

The fields radiated by apertures are non-symmetrical on either side of the aperture, in most practical cases. The fields radiated by the 2-D line source array discussed above are symmetrical on either side of the planar 2-D array. Thus, an obliquity factor of the type $\cos^n \theta/2$ (please refer to the discussion in section II) is included for computing the field radiated by each source in the array. The obliquity factor is different for each n, where $n = 0, \frac{1}{2}, 1, 2$. A function statement FB(SX) computes this obliquity factor for a given value of n. Specifically, the statement concerning FB(SX) reads:

```
FB(SX) = ABS(COS(SX/2.0))**2.0
```

and corresponds to an obliquity factor with n = 2.0. If any other value of n is desired, the appropriate value must be punched into a new card which replaces the previous one. Note that the value of n directly follows the ** symbol in the statement.

The obliquity factor $\cos^n \theta/2$ is plotted as a function of θ for different values of n ($n = \frac{1}{2}$, 1 and 2) in Fig. 17. When the pattern of an isotropic source is multiplied by $\cos^n \theta/2$, it is evident from the resultant pattern that the obliquity factor serves to control the level of the radiation pattern primarily in the range $\pi/3 < \theta < 5\pi/3$. The case n = 0 corresponds to the isotropic case.

E. Instructions for Computing the Incident Field

Two incident field patterns are computed, one is for a phase reference at the center of the aperture, and the other is for a phase reference at Q (see Fig. 7). In the former case, the radiation pattern in dB is designated by DBHA, and is obtained as a function of θ (or TH as defined in the computer program). In the latter case, the radiation pattern in dB is designated by DBGA and is obtained as a function of θ_s (or THS as defined in the computer program). DBGA is computed at a distance equal to R_s from Q. DBHA has been programmed for a range of $R_i + R_s$ from O (center of the aperture as shown in Fig. 7); however, if the user wishes to change the present range for DBHA, only one card in the program deck needs modification. A subroutine designated TEST computes DBHA at a range of $R_i + R_s$ from O; the call statement for this subroutine is

```
CALL TEST (N, AL, RS+RI, A, TYPE)
```

If a different value of the range is desired, one must replace RS+RI in the call statement above by a number which equals the desired value for the range. Note that the new range should have the same unit as those of λ (corresponding to XLAMDA in the computer program).

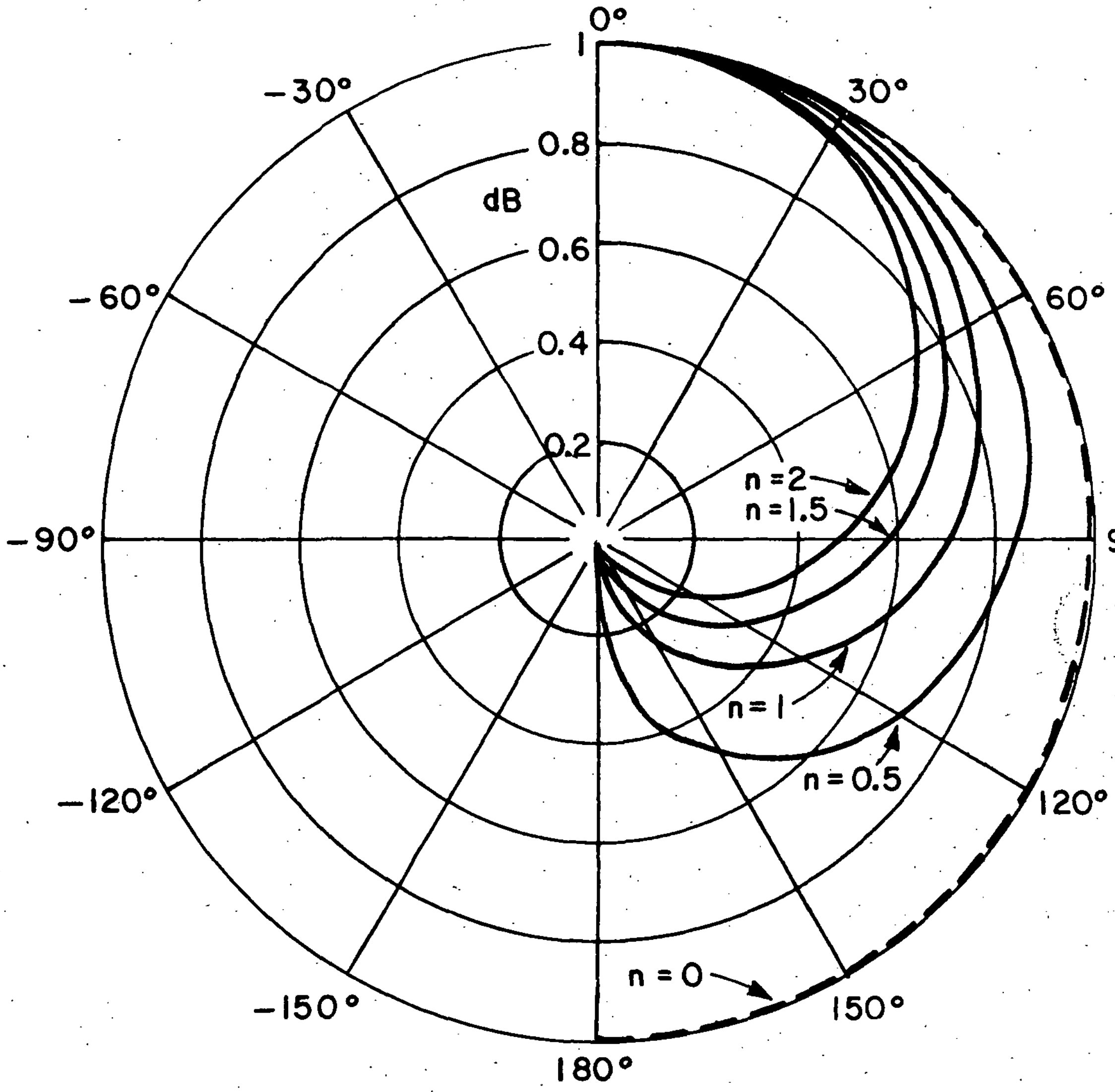

Fig. 17. Patterns of the obliquity factor for different values of n.

F. Sample Programs

In this section, we present a sample case which serves to illustrate the use of our computer program. The example selected involves an array of three magnetic line sources of unit strength which illuminate a rectangular cylinder, as in Fig. 18. We utilize the computer program for calculating the incident field of the array, the field scattered by the 2-D box (rectangular cylinder) and the total field (incident + scattered) surrounding the 2-D box.

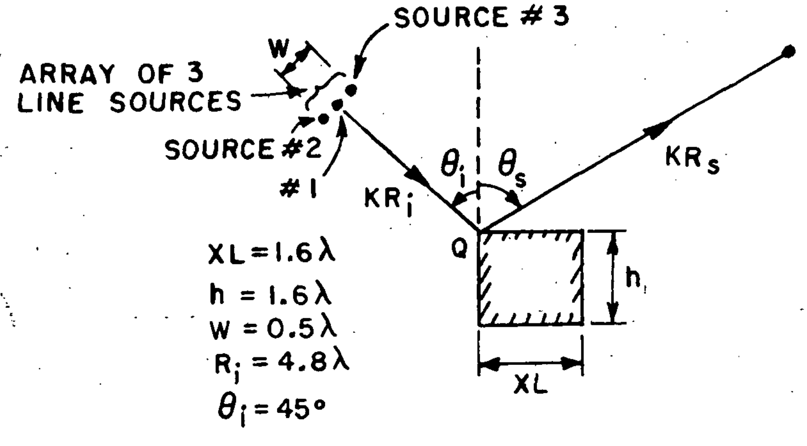

Fig. 18. An array of three line sources in the presence of a square cylinder.

The ordering of the array elements is shown in Fig. 18, where the source at the center is labeled source #1. Note that source #1 corresponds to I = 1, and sources #2 and #3 correspond to I = 2, and I = 3, respectively. For this particular problem, AM(1), AM(2) and AM(3) are each equal to 1.0, and AP(1), AP(2) and AP(3) are each equal to 0.0, because the line sources are of unit strength and zero phase. An obliquity factor corresponding to n = 2 (i.e., obliquity factor = $\cos^2\theta/2$) has been incorporated into the program for the incident field pattern, and the incident field pattern corresponding to DBHA (phase reference at source #1) is plotted in Fig. 19. Also included in Fig. 19 is the incident field pattern without the obliquity factor (n = 0 case) for the sake of comparison. The pattern of the scattered field designated by DBSAS, and computed for values of θ_s (or THS) which lie in the range $-180° \leq \theta_s \leq 180°$, is plotted in Fig. 20. The scattered field obtained by our method is compared against that obtained from a numerical solution to the integral equation for this problem given by J. H. Richmond; these results agree perfectly. Finally, the total field (incident plus scattered, each being phase referenced at Q) is also obtained, and is designated by DBTAL. DBTAL is computed as a function of θ_s (THS in the program) and the results are indicated in Fig. 21 by a dashed curve. The solid curve is added for the sake of comparison; it corresponds to the total field when the incident field has no obliquity factor in it.

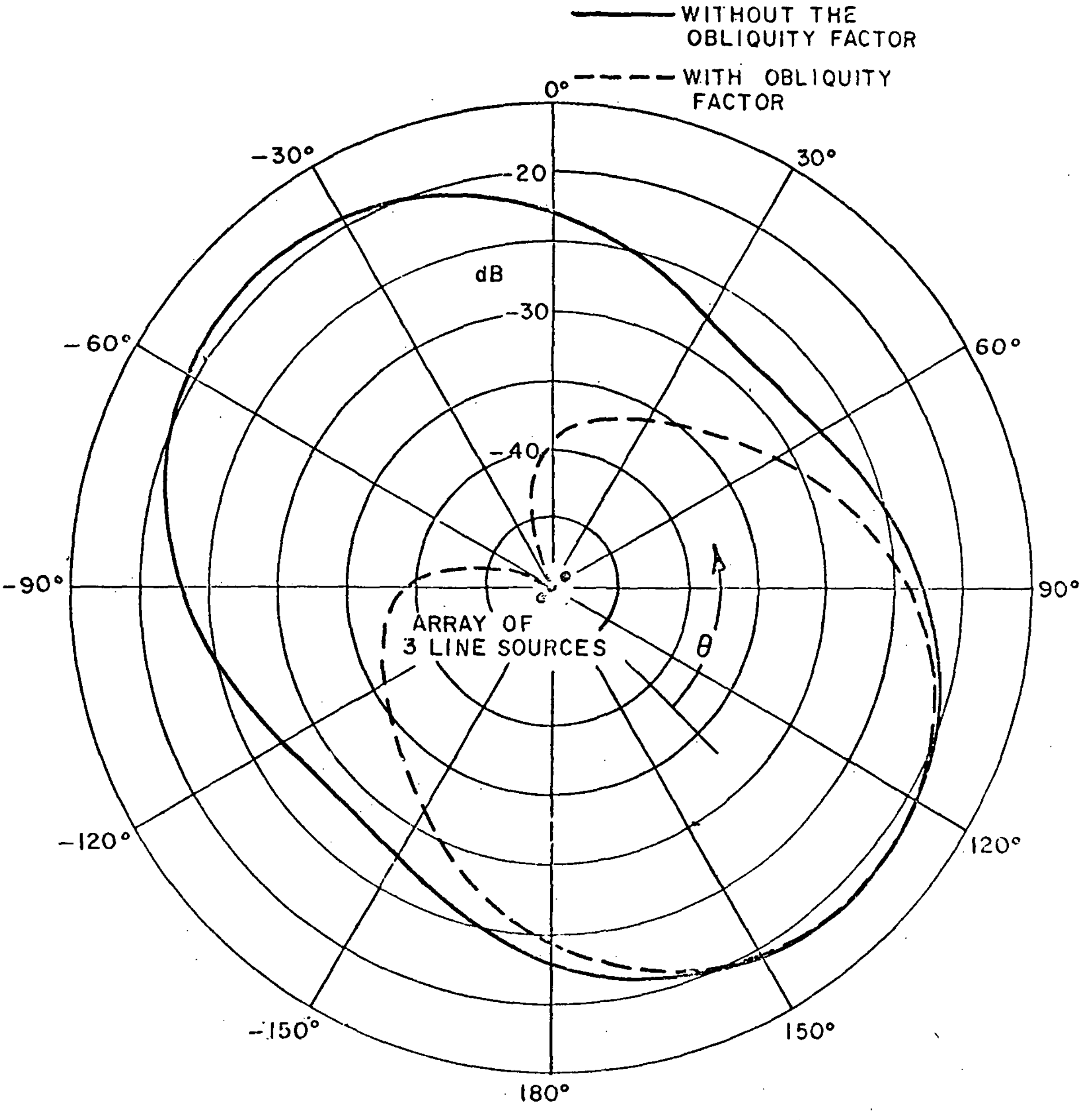

Fig. 19. Patterns of an array of three magnetic line sources of equal strength, with and without the obliquity factor.

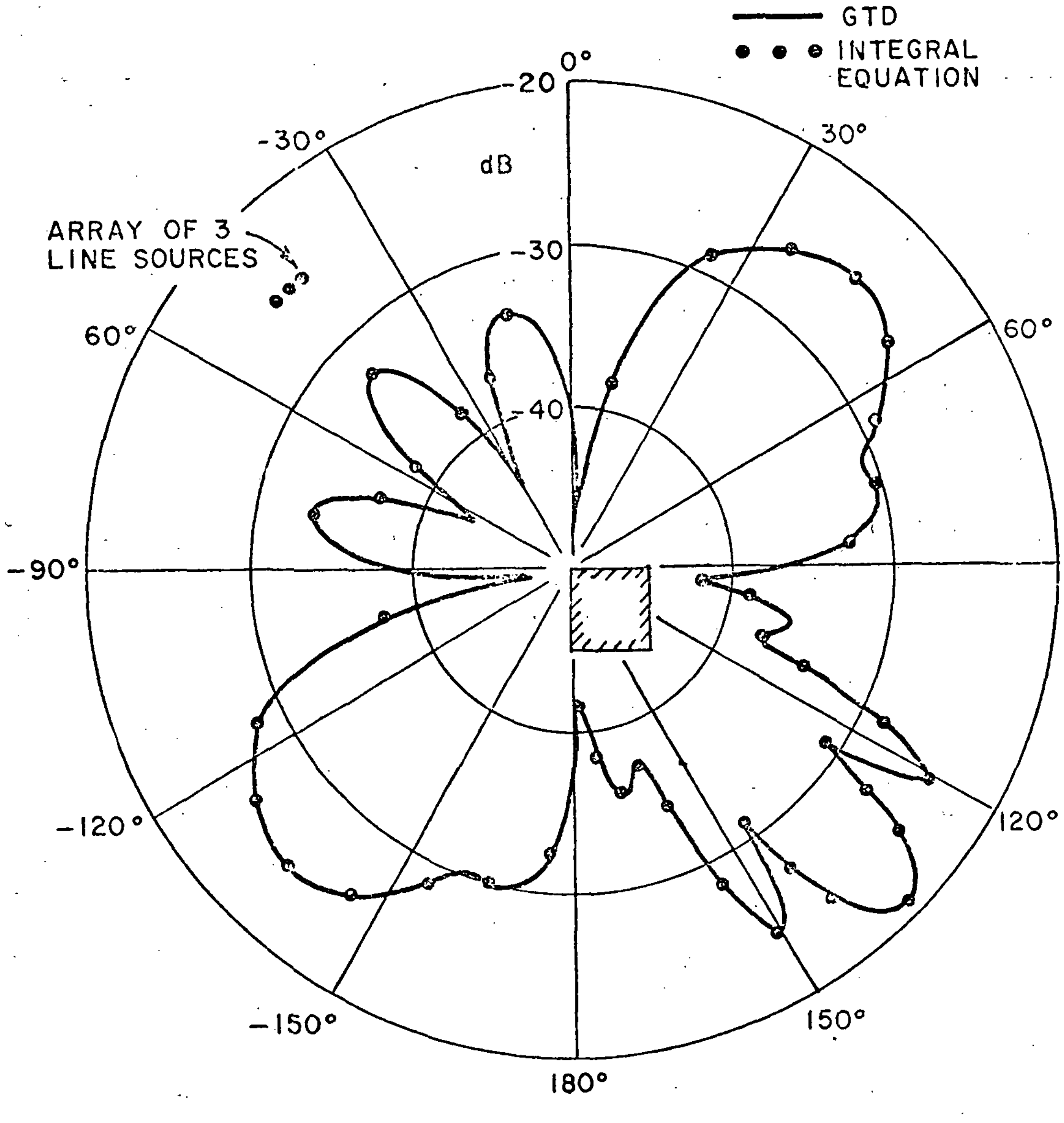

Fig. 20. Pattern of the field scattered by a square cylinder which is illuminated by an array of three magnetic line sources.

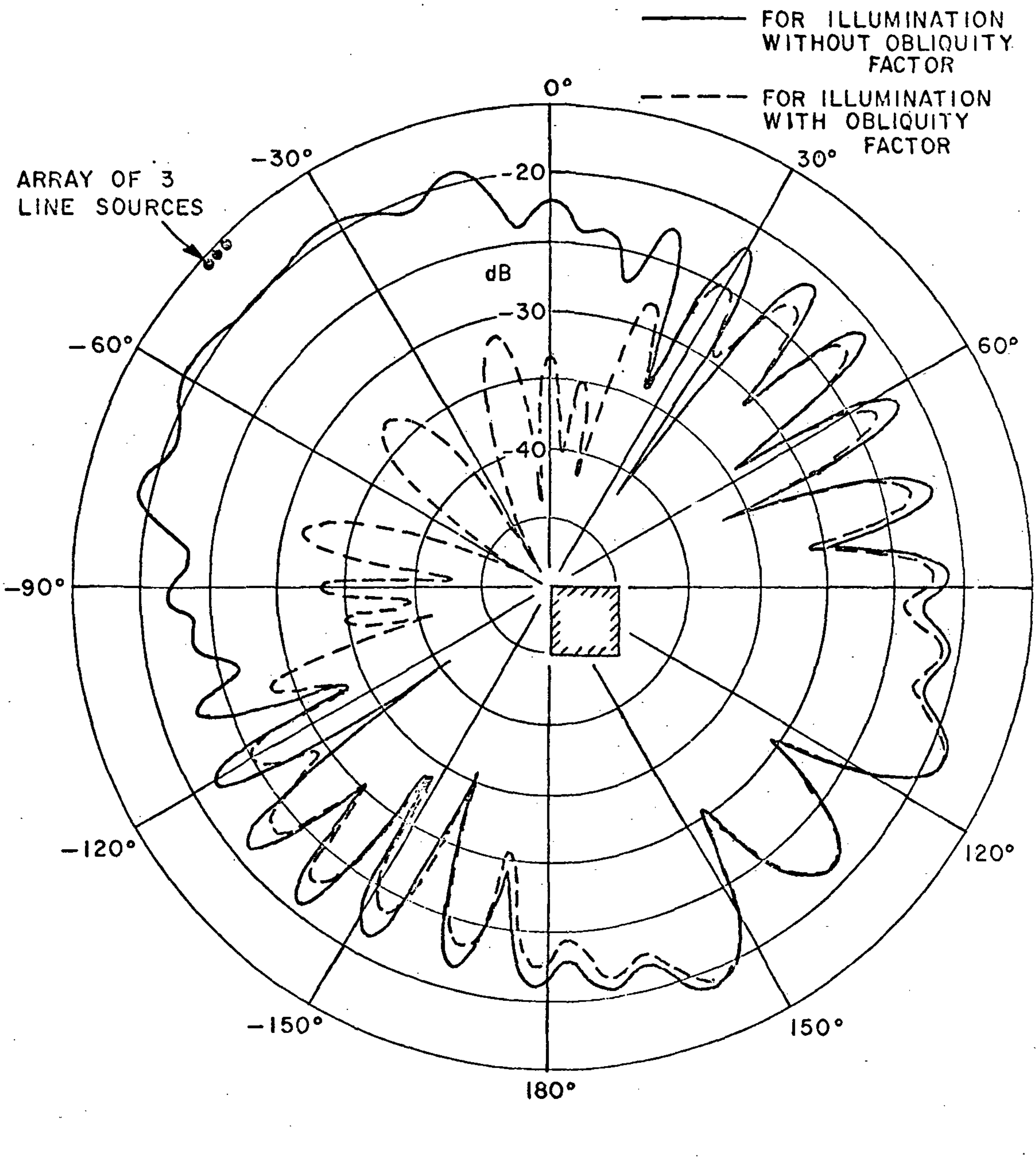

Fig. 21. Pattern of an array of three magnetic line sources in the presence of a square cylinder.

G. Listing of the Computer Programs

```
              PROGRAM LSOSBOX(INPUT,OUTPUT,TAPE5=INPUT,TAPE6=OUTPUT)
          C   PROGRAM LSOSBOX IS PHENIX AUGUST 1972
          C
          C N          THE NUMBER OF LINE SOURCES OR ELEMENTS IN THE ARRAY
          C TYPE       1.0 IS ELECTRIC CURRENT LINE SOURCE
          C TYPE       2.0 IS MAGNETIC CURRENT LINE SOURCE
          C TYPE       3.0 IS MAGNETIC CURRENT MOMENT LINE SOURCE
          C AL         APERTURE WIDTH
          C AM(I)      MAGNITUDE OF THE(I)TH ELEMENT
          C AP(I)      PHASE OF THE(I)TH ELEMENT
          C A(I)       FIELD STRENGTH OF THE(I)TH ELEMENT
          C D(I)       SPACING BETWEEN(I+1)TH AND(I)TH ELEMENTS
          C XLAMDA     TRANSMITTED WAVELENGTH
          C X          THE POINT OF INCIDENCE
          C XL         THE LENGTH OF THE BOX
          C H          THE HEIGHT OF THE BOX
          C RI         INCIDENCE RANGE
          C RS         SCATTERING RANGE
          C THI        ANGLE OF INCIDENCE  0 TO 65
          C THS        ANGLE OF SCATTERING  -65 TO 65
          C XP,YP      OBSERVING POINT
          C XS(I),YS(I)   SOURCE POINT OF THE(I)TH ELEMENT
          C DS         DIFFRACTION COEFFICIENT FOR SOFT BOUNDARY
          C DH         DIFFRACTION COEFFICIENT FOR HARD BOUNDARY
          C GA(I)      DIRECT INCIDENT FIELD DUE TO(I)TH ELEMENT
          C RA(I)      REFLECTED FIELD DUE TO(I)TH ELEMENT
          C DAR1(I)    FIRST ORDER DIFFRACTED FIELD FROM THE RIGHT EDGE DUE TO(I)TH ELEMENT
          C DAR2(I)    2ND   ORDER DIFFRACTED FIELD FROM THE RIGHT EDGE DUE TO(I)TH ELEMENT
          C DAR3(I)    3RD   ORDER DIFFRACTED FIELD FROM THE RIGHT EDGE DUE TO(I)TH ELEMENT
          C DAL1(I)    FIRST ORDER DIFFRACTED FIELD FROM THE LEFT  EDGE DUE TO(I)TH ELEMENT
          C DAL2(I)    2ND   ORDER DIFFRACTED FIELD FROM THE LEFT  EDGE DUE TO(I)TH ELEMENT
          C DAL3(I)    3RD   ORDER DIFFRACTED FIELD FROM THE LEFT  EDGE DUE TO(I)TH ELEMENT
          C TA(I)      THE FIELD AT THE OBSERVING POINT DUE TO(I)TH ELEMENT
          C TOTAL      TOTAL FIELD AT OBSERVING POINT DUE TO ALL THE ELEMENTS
          C DBTAL      MAGNITUDE OF THE TOTAL FIELD EXPRESSED IN  DB
          C DBSAS      MAGNITUDE OF THE SCATTERED FIELD EXPRESSED IN  DB
          C DBHA       DIRECT INCIDENT FIELD EXPRESSED IN  DB
          C PHASE      PHASE OF THE TOTAL FIELD EXPRESSED IN  DEGREES
          C ATAL  AMPLITUDE OF TOTAL FIELD AND ALSO OF INCIDENT FIELD IN SUBROUTINE TEST
          C
000003        DIMENSION  DAL(100)
000003        DIMENSION DAL1(51),DAL2(51),DAL3(51),TA(51)
```

```
000003         DIMENSION  DLR(51),DRL(51)
000003         DIMENSION CALB(51)
000003         DIMENSION DB2(51)
000003         DIMENSION CA(51),RA(51),CAR1(51),DAR2(51),DAR3(51)
000003         DIMENSION GGA(51)
000003         DIMENSION RO(51),OB(51)
000003         DIMENSION SAS(51)
000003         DIMENSION THSTFD(185),AMPTFD(185),CBTFD(185),PHTFD(185)
000003         DIMENSION XS(51),YS(51),AM(51),AP(51),A(51),D(51)
         C
000003         COMPLEX A
000003         COMPLEX  ADDSC(50),CW,CV
000003         COMPLEX  ADDSD(50),CVV,CWW
000003         COMPLEX  CX,CY,CZ,ACCSA(50),ADDSB(50)
000003         COMPLEX CB2,ZP,ZQ,ZR,ZS,DBL1,DBL2
000003         COMPLEX DLL
000003         COMPLEX DR1,DR21,DR22,DR31,DR32,DR33,DL1,DL21,DL22,DL31,DL32,DL33
000003         COMPLEX DX,DY,DS,DZ,GA,RA,DAR1,DAR2,DAR3,DAL1,DAL2,DAL3
000003         COMPLEX F,CA,CB,DC,CD,DE,DF,DG,DH,DI,DJ,DK,DL,DM,DN,DO,DP,DQ,DR
000003         COMPLEX FL,PW,HA,HB,HC,HD,PLUS
000003         COMPLEX GGA
000003         COMPLEX RATAL
000003         COMPLEX SAS
000003         COMPLEX SATAL
000003         COMPLEX TOTAL,U,V,TA
000003         COMPLEX  UU,VV
000003         COMPLEX ZA,ZB,CAL
000003         COMPLEX ZC,ZD,DRL1,DRL2,ZE,ZF,DRL,ZG,ZH,DLR1,DLR2,DLR,ZN,ZM
000003         COMPLEX ZX,ZY,DLB,CALB
         C
000003         COMMON XLAMDA,X,XL,H,RI,RS,THI,UMAX,FIELD,SOURCE
000003         COMMON/PICONST/PI,    TP,STP,SQRTPI,TT,TTDEG,PI02,PI04
         C
000003         FL(X,Y,Z)=2.*CMPLX(0.0,1.0)*SQRT(X)*CEXP(CMPLX(0.0,X))*
              1SQRT(1.5707963267949)*(.5*CMPLX(1.,-1.)-CMPLX(Y,-Z))
000057         PW(X)=CEXP(CMPLX(0.0,-6.2831853071796*X))
000067         COT(X)=COS(X)/SIN(X)
000077         F(Z)=CEXP( CMPLX(0.,-6.2831853071796*Z))/SQRT(6.2831853071795*Z)
000121         DS(UU,VV)=SQRT(6.2831853071796)*(UU-VV)
000142         DH(UU,VV)=SQRT(6.2831853071796)*(UU+VV)
000163         G(W,WW)=W*WW/(W+WW)
000171         FA(SA,SB,SC)= ACOS((SB*SB+SC*SC-SA*SA)/(2.0*SB*SC) )
000206         FB(SX)=ABS(COS(SX/2.0))**2.0
```

```
                C
                C FB(SX) IS THE OBLIQUITY FACTOR.     TO IGNORE IT, SET FB(SX)=1.
                C
000221                CALL PSFJDU
000222                READ(5,1110) N, TYPE,AL,SOURCE
000236           1110 FORMAT(I10,2F10.4,A8)
000236                WRITE(6,2110)N,TYPE,AL,SOURCE
000252           2110 FORMAT(//,3XI2* ELEMENTS*3X*TYPE=  *F3.1,3X*APERTURE WIDTH=*F7.4,3X
                     1A8* CURRENT LINE  SOURCE*/)
000252                READ(5,1114) (  AM(I),AP(I)  ,I=1,N )
000257           1114 FORMAT( 10F8.4 )
000267                PRINT 2114,   (I,AM(I),AP(I)  ,I=1,N )
000305           2114 FORMAT (/15X*AM*10X*AP*/(5X*N(*I2*)=*2F10.4)))
000305                PRINT 8889
000311           8889 FORMAT (1H1)
000311                NNN=N-1
000313                IF(N.EQ.1) GO TO 6666
000314                DO 1000 JJ=1,N
000316                D(JJ)=AL/FLOAT(NNN)
000321           1000 CONTINUE
000323                GO TO 7777
000323           6666 D(1)=0.0
000324           7777 CONTINUE
000324                DO 1115 M=1,N
000326                A(M)=AM(M)*CEXP( CMPLX(0.0,AP(M) )  )
000343                WRITE(6,665) M,A(M)
000354            665 FORMAT(5X, *A(*I2,*)=*,2F10.4)
000354           1115 CONTINUE
000357           6789 CONTINUE
000357                READ(5,1111)XLAMDA,X,XL,H,RI,RS,THI
000401           1111 FORMAT(7F10.4 )
000401                IF(EOF,5)1112,6790
000404           6790 CONTINUE
000404                WRITE(6,2111) XLAMDA,X,XL,H,RI,RS,THI
000426           2111 FORMAT(1H1,5X,*LAMDA= *,F7.4,*  X= *,F7.4,*  L= *,F7.4,*  H= *,
                     1F7.4,*  RI= *,F7.4,*  RS= *,F9.4,*   THI= *,F7.4///// )
                C
000426                PI=3.14159265358 98
000427                TP=2.*PI
000431                STP=SQRT(TP)
000433                SQRTPI=SQRT(PI)
000435                TT=PI/180.
000437                TTDEG=180./PI
```

```
000440          PIL2=0.5*PI
000442          PI04=.25*PI
000443          WLNCRM=1.0/XLAMDA
000445          R=1.0
          C
000446          IF(TYPE.NE.2.C) R=-1.0
000452          XLW=XL/XLAMCA
000453          HW=H/XLAMDA
000455          THI=THI*TT
          *
000457          L=181
          C   L IS 1.GT.THE NUMBER OF POINTS,NPTS, TO BE PLOTTED
          C
000460          THS=181.0
000462          GO TO 9998
          *
000462     9999 CONTINUE
000462          THS=THS*TTDEG
000464          ATAL =0.
000464          CBTAL=0.
000465          DBGA =C.
000466          CBSAS=0.
000467          PHASE=0.
000471          PRINT 4,    THS,ATAL,CBTAL,DBGA,DBSAS,PHASE
000510          IF  ( ATAL.EQ.0.0) GO TO 5
          *
000511     9998 CONTINUE
000511          I=1
000512          THS=THS-2.0
000514          IF(THS.LT.-180.0) GC TO 1
000516          THS=THS*TT
000517          XS(I)=X-RI*SIN(THI)
000525          YS(I)=RI*COS(THI)
000532          XP=X+RS*SIN(THS)
000536          YP=RS*COS(THS)
000541          TE=ATAN2(YP,XP)
000544          TB=ATAN2(YP,XP-XL)
000552       20 CONTINUE
000552          TC=ATAN2(YS(I),XL-XS(I) )
000557          TD=ATAN2(YS(I),-XS(I) )
          *
000564          BOND=0.01*TT
          *
```

```
000566          IF( ABS(TE-PIO2  ).LE.BOND ) GO TO  9999
000573          IF( ABS(TB-PIO2  ).LE.BCND ) GO TO  9999
000577          IF( ABS(TB-TC).LE.BOND ) GO TO 9999
000603          IF( ABS(TE-TD).LE.BCND ) GO TO 9999
        *
        C     ANY ONE OF THE 11 IF STATEMENTS ENDING IN GO TO 9999 MAY CAUSE THE
        C        CURRENT ODD NUMBERED THS ANGLE IN DEG TO BE SKIPPED
        C
000607          XR=(XP*YS(I)+XS(I)*YP)/(YS(I)+YP )
000616          RO(I)=SQFT((XP-XS(I))*(XP-XS(I))+(YP-YS(I))*(YP-YS(I)))/XLAMDA
000633          OB(I)=PI
000634          IF(ABS(THS+THI).GT.BCND) OB(I)=FA(RS,RI,RO(I)*XLAMDA)
000647          R1=WLNORM    *SQRT( (XR-XS(I))*(XR-XS(I))+(-YS(I))*(-YS(I))  )
000660          R2=WLNCRM    *SQRT(   (XP-XR)*(XP-XR)+(YP*YP) )
000667          R3=WLNORM    *SQRT( (XL-XS(I))*(XL-XS(I))+(-YS(I))*(-YS(I)) )
000701          R4=WLNORM    *SQRT( (XP-XL)*(XP-XL)+(YP*YP) )
000710          R5=WLNCRM    *SQRT ( (XP-XL)*(XP-XL)+(YP+H )*(YP+H ) )
000721          R6=WLNORM    *SQRT( (-XS(I))*(-XS(I))+(-YS(I))*(-YS(I)) )
000732          R7=WLNCRM    *SQRT ( (XP*XP)+(YP*YP) )
000740          R8=WLNORM    *SQRT( (XP*XP)+(YP+H )*(YP+H ) )
000747          THR=ATAN2(YP,XP-XR)
000754          R9=WLNORM    *SQRT(XS(I)*XS(I)+(YS(I)+H)*(YS(I)+H) )
000765          PHP=(PI-ATAN2( YS(I),XS(I)-XL ) )*TTDEG
000774          PH1=(PI-ATAN2(YP,XP-XL))*TTDEG
001003          PH2=(PI-ATAN2(XP-XL,-H-YP))*TTDEG
001014          PH3=270.0-PH1
001016          THP=(ATAN2(YS(I),XS(I))  )*TTDEG
001022          TH1=(PI-ATAN2(YP,-XP))*TTDEG
001030          TH2=(PI-ATAN2(-XP,-H-YP))*TTDEG
001041          TH3=270.0-TH1
001043          TH4=ATAN2(-XS(I),YS(I)+H)
        C
001052          IF(XS(I).LT.0.0.AND.ABS((THI-THS)/TT-180.0).LE.1.0) GO TO 9999
001067          IF(XS(I).GE.0.0.AND.ABS(TH1-THP-180.0).EQ.0.0) GO TO 9999
001101          IF(XS(I).LT.0.0.AND.ABS(TH2-TH4/TT-180.0).EQ.0.0) GO TO 9999
001113          IF(ABS(PH1-PHP-180.0).EQ.0.0) GO TO 9999
        C
001116          QA=G(R3,R4 )
001121          CALL DFRC=(DA,1.5,QA,PH1-PHP, 1.)
001126          CALL DFRCF(DB,1.5,QA,PH1+PHP, 1.)
001134          DR1 =DH(DA,DB)
        **
        **
```

```
001143      IF( TYPE.NE.2.0)  DR1=DS(DA,DB)                         21500000
001154      QB=G(R3,HW)                                             21600000
001157      CALL DFRCF(DC,1.5,QB,270.00-PHP,1. )                    21700000
001164      CALL DFRCF(DD,1.5,QB,270.00+PHP,1. )                    21800000
001172      DR21=DH(DC,DD)                                          21900000
001201      IF(TYPE.NE.2.0) DR21=DS(DC,DD)                          22000000
001212      QC=G(HW,R5)                                             22100000
001215      CALL DFRCF(DE,1.5,QC,PH2+0.0,1. )                       22200000
001222      CALL DFRCF(DF,1.5,QC,PH2-0.0,1.)                        22300000
001230      DR22=DH(DE,DF)                                          22400000
001237      IF( TYPE.NE.2.0) DR22=DS(DE,DF)                         22500000
001250      DR31=DR21                                               22600000
001253      CALL DFRCF(DG,1.5,HW,0.0,1.0 )                          22700000
001256      CALL DFRCF(DZ,1.5,HW,0.0,1.0 )                          22800000
001262      DR32=DH(DG,DZ)                                          22900000
001271      IF( TYPE.NE.2.0) DR32=DS(DG,DZ)                         23000000
001302      QD=G(HW,R4)                                             23100000
001305      CALL DFRCF(DI,1.5,QD,PH3,1.0 )                          23200000
001310      CALL DFRCF(DJ,1.5,QD,PH3,1.0 )                          23300000
001314      DR33=DH(DI,DJ)                                          23400000
001323      IF(TYPE.NE.2.0) DR33=DS(DI,DJ)                          23500000
001334      QE=G(R6,R7)                                             23600000
001337      CALL DFRCF(DK,1.5,QE,TH1-THP,1.0 )                      23700000
001344      CALL DFRCF(DL,1.5,QE,TH1+THP,1.0 )                      23800000
001352      DL1  =DH(DK,DL)                                         23900000
001361      IF( TYPE.NE.2.0)  DL1=DS(DK,DL)                         24000000
001372      QF=G(R6,HW)                                             24100000
001375      CALL DFRCF(DM,1.5,QF,270.00-THP,1.0 )                   24200000
001402      CALL DFRCF(DN,1.5,QF,270.00+THP,1.0 )                   24300000
001410      DL21=DH(DM,DN)                                          24400000
001417      IF(TYPE.NE.2.0) DL21=DS(DM,DN)                          24500000
001430      QG=G(HW,R8)                                             24600000
001433      CALL DFRCF(DO,1.5,QG,TH2,1.0 )                          24700000
001436      CALL DFRCF(DP,1.5,QG,TH2,1.0 )                          24800000
001442      DL22=DH(DO,DP)                                          24900000
001451      IF(TYPE.NE.2.0) DL22=DS(DO,DP)                          25000000
001462      DL31=DL21                                               25100000
001465      CALL DFRCF(DQ,1.5,HW,0.0,1.0 )                          25200000
001470      CALL DFRCF(DR,1.5,HW,0.0,1.0 )                          25300000
001474      DL32=DH(DQ,DR)                                          25400000
001503      IF( TYPE.NE.2.0) DL32=DS(DQ,DR)                         25500000
001514      QI=G(HW,R7)                                             25600000
001517      CALL DFRCF(DX,1.5,QI,TH3,1.0 )                          25700000
```

```
               CALL DFRCF(DY,1.5,QI,TH3,1.0 )
001525         DL33=DF(DX,DY)
001535         IF(TYPE.NE.2.0) DL33=DS(DX,DY)
001546         QK=G(R8,R9)
001551         CALL DFRCF(ZA,1.5,QK,TH2-TH4/TT,1.0)
001557         CALL DFRCF(ZB,1.5,QK,TH2+TH4/TT,1.0)
001566         DLL=DH(ZA,ZB)
001575         IF(TYPE.NE.2.0)  DLL=DS(ZA,ZB)
001606         DAL(I)=A(I)*F(R9)*DLL*F(R8)
001632         DAL(I)=DAL(I)*FB(THI-TH4)
001642         GA(I)=A(I)*F(RO(I))
001655         GA(I)=GA(I)*FB(CB(I))
001665         RA(I)=A(I)*R*F(R1+R2)
001701         RA(I)=RA(I)*FB(THI-ATAN2(YS(I),ABS(XR-XS(I))))
001717         DAR1(I)=A(I)*F(R3)*DR1*F(R4)
001743         DAR1(I)=DAR1(I)*FB(0.5*PI-THI-PHP*TT)
001756         DAR2(I)=A(I)*F(R3)*DR21*F(HW)*0.5*DR22*F(R5)
002014         DAR2(I)=DAR2(I)*FB(0.5*PI-THI-PHP*TT)
002027         DAL1(I) =A(I)*F(R6)*DL1*F(R7)
002053         DAL1(I)=DAL1(I)*FB(0.5*PI+THI-THP*TT)
002066         DAL2(I)=A(I)*F(R6)*DL21*F(HW)*0.5*DL22*F(R8)
002124         DAL2(I)=DAL2(I)*FB(0.5*PI+THI-THP*TT)
002137         IF(XS(I).EQ.0.0) DAL2(I)=0.5*DAL(I)
002147         YL2=G(R8,R6+H)
002153         XF=2.0*G(R6,H+R8)
002161         CALL CS(C,S,XF)
002163         CALL WANG(TH2,0.0,1.5,YL2,HA,HB)
002167         CALL WANG(270.0,0.0,1.5,YL2,HC,HD)
002173         PLUS=A(I)*F(R6)*FL(XF,C,S)*COT(TP/3.0)*PW(0.125)*F(HW)/3.0/STP
002243         IF(TYPE.NE.2.0) HA=HB
002247         IF(XS(I).EQ.0.0) DAL2(I)=DAL2(I)-PLUS*HA*F(R8)
          C
002270         IF(XS(I).EQ.0.0.AND.TYPE.EQ.1.0) DAL2(I)=CMPLX(0.0,0.0)
002306         IF(XS(I).GE.0.0) DAL(I)=CMPLX(0.0,0.0)
          C
002316         DAL3(I)=CMPLX(0.0,0.0)
002325         DAR3(I)=CMPLX(0.0,0.0)
          C
002333         WX=G(R9,HW)
002335         CALL DFRCF(ZX,1.5,WX,0.0-TH4/TT,1.0)
002343         CALL DFRCF(ZY,1.5,WX,0.0+TH4/TT,1.0)
002352         DLB=DH(ZX,ZY)
002361         IF(TYPE.NE.2.0)  DLB=DS(ZX,ZY)
```

```
002372          DALB(I)=A(I)*F(R9)*DLB*0.5*F(HW)*DL33*F(R7)
002430          DALB(I)=DALB(I)*FB(THI-TH4)
002440          IF(XS(I).GT.0.0) DALB(I)=CMPLX(0.0,0.0)
00245           IF(THI.GT.270..AND.THI.LT.360.) DALB(I)=CMPLX(0.0,0.0)
       C
002467          R10=SQRT((XP-XL)*(XP-XL)+(YP+H)*(YP+H))/XLAMDA
002500          TH5=(PI-ATAN2(-YP,XP-XL))*TTDEG
002510          PA=G(R9,XLW)
002513          CALL DFRCF(ZP,1.5,PA,270.0-TH4/TT,1.0)
002521          CALL DFRCF(ZQ,1.5,PA,270.0+TH4/TT,1.0)
002530          DBL1=DH(ZP,ZQ)
002537          IF(TYPE.NE.2.0) DBL1=DS(ZP,ZQ)
002550          PB=G(XLW,R10)
002553          CALL DFRCF(ZR,1.5,PB,0.0-TH5,1.0)
002560          CALL DFRCF(ZS,1.5,PB,0.0+TH5,1.0)
002566          DBL2=DH(ZR,ZS)
002575          IF(TYPE.NE.2.0) DBL2=DS(ZR,ZS)
002606          DB2(I)=A(I)*F(R9)*DBL1*F(XLW)*0.5*DBL2*F(R10)
002644          DB2(I)=DB2(I)*FB(THI-TH4)
002654          IF(XS(I).GT.0.0) DB2(I)=CMPLX(0.0,0.0)
002664          IF(XS(I).EQ.0.0) DB2(I)=0.5*DB2(I)
002674          IF(TYPE.NE.2.0) HC=HD
002701          IF(XS(I).EQ.0.0) DB2(I)=DB2(I)-PLUS*HC*F(XLW)*DBL2*F(R10)
002733          IF(TH5.GT.270.0.AND.TH5.LT.360.0) DB2(I)=CMPLX(0.0,0.0)
002752          QX=G(R3,XLW)
002755          CALL DFRCF(ZG,1.5,QX,0.0-PHP,1.0)
002762          CALL DFRCF(ZH,1.5,QX,0.0+PHP,1.0)
002770          DLR1=DH(ZG,ZH)
002777          IF(TYPE.NE.2.0) DLR1=DS(ZG,ZH)
003010          QW=G(R7,XLW)
003013          CALL DFRC=(ZM,1.5,CW,THI,1.0)
003016          CALL DFRCF(ZN,1.5,QW,THI,1.0)
003022          DLR2=DH(ZM,ZN)
003031          IF(TYPE.NE.2.0) DLR2=DS(ZM,ZN)
003042          DLR(I)=A(I)*F(R3)*DLR1*F(XLW)*0.5*DLR2*F(R7)
003100          DLR(I)=DLR(I)*FB(0.5*PI-THI-PHP*TT)
003113          IF(THI.GE.270.0.AND.THI.LT.360.) DLR(I)=CMPLX(0.0,0.0)
003131          QZ=G(R6,XLW)
003134          CALL DFRCF(ZC,1.5,QZ,0.0-THP,1.0)
003141          CALL DFRCF(ZD,1.5,QZ,0.0+THP,1.0)
003147          DRL1=DH(ZC,ZD)
003156          IF(TYPE.NE.2.0) DRL1=DS(ZC,ZD)
003157          QY=G(XLW,R4)
```

```
003172          CALL DFRCF(ZE,1.5,QY,PHL,1.0)
003175          CALL DFRCF(ZF,1.5,CY,PH1,1.0)
003201          DRL2=DH(ZF,ZF)
003210          IF(TYPE.NE.2.0) DRL2=CS(ZE,ZF)
         **
         **
003221          DRL(I)=A(I)*F(R6)*DRL1*F(XLW)*0.5*DRL2*F(R4)
003257          DRL(I)=DRL(I)*FB(0.5*PI+THI-THP*TT)
003272          IF(PHL.GE.270.0.AND.PH1.LT.360.) DRL(I)=CMPLX(0.0,0.0)
003310          ADDSA(I)=CMPLX(0.0,C.0)
003317          CALL KKDC(CX,1.5,QK,0.0,TH2,1.0,1)
         *
         *
003325          IF(TYPE.EQ.1.0.AND.TH2.GT.0.0.AND.TH2.LT.270.0.AND.XS(I).EQ.0.0)
               1ADDSA(I)=A(I)*F(R9)*0.5*SQRT(TP)*CX*F(R8)/CMPLX(0.0,R9*TP)*2.0
003406          ADDSB(I)=CMPLX(0.0,C.0)
003415          CALL KKDC(CY,1.5,QB,PHP,270.0,1.0,0)
003423          CALL KKDC(CZ,1.5,QC,0.0,270.0-TH5,1.0,1)
003434          IF(TYPE.EQ.1.0.AND.TH5.GT.0.0.AND.TH5.LT.270.0)
               1ADDSB(I)=A(I)*F(R3)*F(HW)*CY*TP*0.5*CZ*F(R10)/CMPLX(0.0,HW*TP)
003515          ADDSC(I)=CMPLX(0.0,0.0)
003524          CALL KKDC(CV,1.5,QF,90.0,270.0,1.0,0)
003532          CALL KKDC(CW,1.5,QG,0.0,TH2,1.0,1)
003541          IF(TYPE.EQ.1.0.AND.TH2.GT.0.0.AND.TH2.LT.270.0.AND.XS(I).EQ.0.0)
               1ADDSC(I)=A(I)*F(R6)*CV*F(HW)*0.5*CW*F(R8)/CMPLX(0.0,TP*HW)
003626          ADDSC(I)=ADDSC(I)*TP
003633          ADDSD(I)=CMPLX(0.0,0.0)
003642          CALL KKDC(CVV,1.5,QX,PHP,0.0,1.0,0)
003650          CALL KKDC(CWW,1.5,QW,0.0,TH1,1.0,1)
003657          IF(TYPE.EQ.1.0.AND.TH1.GT.0.0.AND.TH1.LT.270.0)
               1ADDSD(I)=A(I)*F(R3)*CVV*F(XLW)*0.5*CWW*F(R7)/CMPLX(0.0,XLW*TP)
         *
         *
003737          ADDSC(I)=ADDSD(I)*TP
         ***
003744          IF(TYPE.EQ.3.0.AND.OB(I).LT.PI/2.0) GA(I)=GA(I)*COS(OB(I))
003765          IF(TYPE.EQ.3.0.AND.CB(I).GT.PI/2.0) GA(I)=GA(I)*COS(PI-OB(I))
004011          GGA(I)=GA(I)
004015          IF(TYPE.EQ.3.0)   RA(I)=RA(I)*COS(THI-ATAN2(YS(I),ABS(XR-XS(I))))
004037          IF(TYPE.EQ.3.0)   DAL(I)=DAL(I)*COS(THI-TH4)
004053          IF(TYPE.EQ.3.0) DAR1(I)=DAR1(I)*COS(0.5*PI-THI-PHP*TT)
004072          IF(TYPE.EQ.3.0) DAR2(I)=DAR2(I)*COS(0.5*PI-THI-PHP*TT)
004111          IF(TYPE.EQ.3.0) DAL1(I)=DAL1(I)*CCS(0.5*PI+THI-THP*TT)
```

```
004130       IF(TYPE.EQ.3.0) DAL2(I)=DAL2(I)*COS(0.5*PI+THI-THP*TT)
004147       IF(TYPE.EQ.3.0) DALB(I)=DALB(I)*COS(THI-TH4)
004163       IF(TYPE.EQ.3.0)  DB2(I)= DB2(I)*COS(THI-TH4)
004177       IF(TYPE.EQ.3.0)  DLR(I)=DLR(I)*COS(0.5*PI-THI-PHP*TT)
004216       IF(TYPE.EQ.3.0)  DRL(I)=DRL(I)*COS(0.5*PI+THI-THP*TT)
       ***
004235       IF(YP.GT.0.0) GO TO 3333
004240       RA(I)=CMPLX(0.0,0.0)
       *
004246       IF(XS(I).GE.0.0.AND.PH1-PHP.EQ.180.0.OR .TH1-THP.EQ.180.)
            1 GO TO 9999
       *
004264       IF(XS(I).GE.0.0.AND.PH1-PHP.GE.180.0.AND.TH1-THP.GE.180.)GA(I)=
            1CMPLX(0.0,0.0)
       *
004312       IF(XS(I).LT.0.0.AND.PH1-PHP.EQ.180.0.OR .(TH2-TH4/TT).EQ.180.0)
            1 GO TO 9999
       *
004331       IF(XS(I).LT.0.0.AND.PH1-PHP.GT.180.0.AND.(TH2-TH4/TT).GT.180.0)
            1 GA(I)=CMPLX(0.0,0.0)
004356       IF(PH1.GT.270.0.AND.PH1.LT.360.0) CAR1(I)=CMPLX(0.0,0.0)
004375       IF(TH1.GT.270.0.AND.TH1.LT.360.0) DAL1(I)=CMPLX(0.0,0.0)
004414       IF(PH2.GE.270.0.AND.PH2.LT.360.0) CAR2(I)=CMPLX(0.0,0.0)
004433       IF(TH2.GE.270.0.AND.TH2.LT.360.0) CAL2(I)=CMPLX(0.0,0.0)
004452       IF(TH3.LE.0.0) DAL3(I)=CMPLX(0.0,0.0)
004463       IF(PH3.LE.0.0) DAR3(I)=CMPLX(0.0,0.0)
004474       IF(TH2.GE.270.0.AND.TH2.LT.360.0) DAL(I)=CMPLX(0.0,0.0)
004513       IF(XS(I).LT.0.0.AND.XP.LT.0.0) RA(I)=A(I)*R*F(SQRT((XS(I)+XP)*
            1(XS(I)+XP)+(YS(I)-YP)*(YS(I)-YP))/XLAMDA)
004550       YR=YP-XP*(YP-YS(I))/(XP+XS(I))
       *
004557       IF(YR.EQ.-H.OR.YR.EQ.0.0) GO TO 9999
       *
004566       IF(XS(I).LT.0.0.AND.XP.LT.0.0)
            1RA(I)=RA(I)*FB(ATAN2(-XS(I),YS(I)-YR)-THI)
004612       IF(XS(I).LT.0.0.AND.XP.LT.0.0.AND.TYPE.EQ.3.0)
            1RA(I)=RA(I)*COS(THI-ATAN2(-XS(I),YS(I)-YR))
004645       IF(YR.LE.-H.OR.YR.GE.0.0) RA(I)=CMPLX(0.0,0.0)
004664       TA(I)=GA(I)+RA(I)+CAR1(I)+DAR2(I)+DAR3(I)+DAL1(I)+DAL2(I)+DAL3(I)
            1+DAL(I)
004723       TA(I)=TA(I)+DLR(I)+DRL(I)
004734       TA(I)=TA(I)+DB2(I)
004742       TA(I)=TA(I)+DALB(I)
```

```
[illegible]           SAS(I)=TA(I)-GA(I)
004757                TA(I)=TA(I)+ADDSA(I)
004765                TA(I)=TA(I)+ADDSB(I)
004773                TA(I)=TA(I)+ADDSC(I)
005001                TA(I)=TA(I)+ADDSD(I)
005007                GO TO 4444
005007          3333  CONTINUE
005007                TA(I)=GA(I)+RA(I)+DAR1(I)+DAR2(I)+DAR3(I)+DAL1(I)+DAL2(I)+DAL3(I)
005042                TA(I)=TA(I)+DLR(I)+CRL(I)
005053                TA(I)=TA(I)+DB2(I)
005061                TA(I)=TA(I)+DALB(I)
005067                TA(I)=TA(I)+ADDSA(I)
005075                TA(I)=TA(I)+ADDSB(I)
005103                TA(I)=TA(I)+ADDSC(I)
005111                TA(I)=TA(I)+ADDSD(I)
005117                IF(XP.GT.XL.AND.TB.LT.TC) TA(I)=TA(I)-RA(I)-DAL2(I)
005141                IF(XS(I).GT.0.0.AND.XP.GT.XL.AND.TB.GT.TC) TA(I)=TA(I)-DAL2(I)
005164                IF(XS(I).GT.0.0.AND.XP.LT.XL.AND.XP.GT.0.0) TA(I)=TA(I)-DAL2(I)
                     1-DAR2(I)
005211                IF(XS(I).GT.0.0.AND.XP.LT.0.0.AND.TE.LT.TD) TA(I)=TA(I)-DAR2(I)
005233                IF(XS(I).GT.0.0.AND.XP.LT.0.0.AND.TE.GT.TD) TA(I)=TA(I)-DAR2(I)
                     1-RA(I)
005260                IF(XS(I).EQ.0.0.AND.XP.GT.XL.AND.TB.GT.TC) TA(I)=TA(I)-DAL2(I)
005303                IF(XS(I).EQ.0.0.AND.XP.LT.XL.AND.XP.GT.0.0) TA(I)=TA(I)-DAL2(I)
                     1-DAR2(I)
005330                IF(XS(I).EQ.0.0.AND.XP.LT.0.0) TA(I)=TA(I)-RA(I)-DAR2(I)
005350                IF(XS(I).LT.0.0.AND.XP.GT.XL.AND.TB.GT.TC.AND.TE.LT.TD) TA(I)=
                     1TA(I)-DAL2(I)
005402                IF(XS(I).LT.0.0.AND.XP.GT.XL.AND.TB.GT.TC.AND.TE.GT.TD) TA(I)=
                     1TA(I)-RA(I)-DAL2(I)
005437                IF(XS(I).LT.0.0.AND.XP.LT.XL.AND.XP.GT.0.0.AND.TE.LT.TD) TA(I)=
                     1TA(I)-DAL2(I)-DAR2(I)
005471                IF(XS(I).LT.0.0.AND.XP.LT.XL.AND.XP.GT.0.0.AND.TE.GT.TD) TA(I)=
                     1TA(I)-RA(I)-DAL2(I)-DAR2(I)
005526                IF(XS(I).LT.0.0.AND.XP.LT.0.0) TA(I)=TA(I)-RA(I)-DAR2(I)+DAL(I)
005551                SAS(I)=TA(I)-GA(I)
005560          4444  CONTINUE
005560                NN=(N-1)/2
005562                II=I-NN
005564                IF(I.EQ.N) GO TO 11
005566                XS(I+1)=XS(1)-FLOAT(I)*D(I)*COS(THI)
005575                IF(I.GT.NN) XS(I+1)=XS(1)+FLOAT(II)*D(I)*COS(THI)
005606                YS(I+1)=YS(1)-FLOAT(I)*D(I)*SIN(THI)
```

```
          IF(I.GT.NNN) YS(I+1)=YS(1)+FLOAT(I1)*D(1)*SIN(TH1)
005626    M=I+1
005630    RO(M)=SQRT((XP-XS(M))*(XP-XS(M))+(YP-YS(M))*(YP-YS(M)))/XLAMDA
005644    OB(M)=    FA(D(I)*FLOAT(I),RO(1)*XLAMDA,RO(M)*XLAMDA)+OB(1)
005655    IF(I.GT.NN) OB(M)=OB(1)-FA(FLOAT(I-NN)*D(I),RO(1)*XLAMDA,
         1RO(M)*XLAMDA)
005672    IF(OB(1).GT.PIO2  ) OB(M)=OB(1)-FA(D(I)*FLOAT(I),RO(1)*XLAMDA,
         1RO(M)*XLAMDA)
005707    IF(OB(1).GT.PIO2   .AND.I.GT.NN)
         1OB(M)=OB(1)+FA(FLOAT(I-NN)*D(I),RO(1)*XLAMDA,RO(M)*XLAMDA)
005734    IF(I.GT.NNN) GO TO 11
005740    I=I+1
005741    GO TO 20
005741 11 CONTINUE
005741    SATAL=CMPLX(0.0,0.0)
005744    RATAL=CMPLX(0.0,0.0)
005746    TOTAL=CMPLX(0.0,0.0)
005751    DO 3 K=1,N
005752    RATAL=RATAL+GGA(K)
005760    SATAL=SATAL+SAS(K)
005766  3 TOTAL=TOTAL+TA(K)
005776    ATAL=CABS(TOTAL)
006000    DBTAL=20.0*ALOG10(ATAL)
006003    GAM=CABS(RATAL)
006005    DBGA=20.0*ALOG10(GAM)
006010    SASM=CABS(SATAL)
006012    DBSAS=20.0*ALOG10(SASM)
006015    WR=REAL(TOTAL)
006017    WI=AIMAG(TOTAL)
006020    PHASE=ATAN2(WI,WR)
006023    THS = THS*TTDEG
006025    PHASE=PHASE*TTDEG
006027    WRITE(6,4) THS,ATAL,DBTAL,DBGA,DBSAS,PHASE
006046  4 FORMAT(5X,*THS=*,F7.2,5X,*ATAL=*,E12.4,5X,*DBTAL=*,E12.4,5X,
         1*DBGA=*,E12.4,5X,*DBSAS=*,E12.4,5X*PHASE=*E12.4)
       *
       C L-1 STORES THE COMPUTED POINTS IN REVERSE ORDER IN THE ARRAY, THAT IS,
       C      THS FROM -179 TO +179 DEG FOR CARTESIAN PLOTTING
       C
       *
006046  5 L=L-1
006050    THSTFD(L)=THS
006052    AMPTFD(L)=ATAL
```

```
006053          CBTFD(L)=DBTAL
CC6055          PHTFD(L)=PHASE
006056          GO TO 9998
        *
006057        1 CONTINUE
        C     FIND MAX AMPTFD
006057          AMAX=AMPTFD(1)
CC606J          TMAX=THSTFD(1)
006052          DO 6956 J=2,180
0C6064          IF (AMPTFD(J).EQ.0.)  AMPTFD(J)=(AMPTFD(J-1)+AMPTFD(J+1))/2.
006070          IF (AMPTFD(J).LE.AMAX) GO TO 6956
006073          AMAX=AMPTFD(J)
CC6074          TMAX=THSTFD(J)
006076     6956 CONTINUE
        *
        C     NORMALIZE AMPTFD
CC6100          DO 6957 J=1,180
006102          AMPTFD(J)=AMPTFD(J)/AMAX
CC6104     6957 CONTINUE
006106          PRINT 5553,AMAX,TMAX
0C6115     5553 FORMAT(//* MAX AMPTFD=*F9.5* FOR THSTFD=*F3* DEG*)
        *
0C6115          PRINT 29,(THSTFD(J),AMPTFD(J),DBTFD(J),PHTFD(J), J=1,180)
006135       29 FORMAT(///2X*THS*5X*AMPTFDNOR*7X*DBTFD*8X*PHASE*/(F5,3(4XF10.5)))
        *
006135          THSTFD(181)=-180.
006136          THSTFD(182)=30.
006140          AMPTFD(181)=0.
CC6140          AMPTFD(182)=.1
006142          PHTFD(181)=-180.
006142          PHTFD(182)=30.
006144          CALL PLTTFDP(THSTFD,PHTFD,180)
0C6146          CALL PLTTFD(THSTFD,AMPTFD,180)
        *
        *
        *
        C   REORDER THSTFD VS DBTFD IN THE ARRAY,FROM 1 TO 359 DEG,FOR POLAR PLOT
        *
006151          KK=90
0C6152          DO 1113 J=1,90
006154          KK=KK+1
006156          TEMP=THSTFD(KK)
006157          THSTFD(KK)=THSTFD(J)+360
```

```
006162          THSTFD(J)=TEMP
006164          TEMP=CBTFD(KK)
006165          DBTFD(KK)=DBTFD(J)
006167          DBTFD(J)=TEMP
006170     1113 CONTINUE
          **    IN LSCSBOX
          *
006172          FIELD=5HTOTAL
006173          DMAX=DBTFD(1)
006174          TMAX=THSTFD(1)
006176          DO 6958 J=2,180
006200          IF (DBTFD(J).EQ.0.) DBTFD(J)=(DBTFD(J-1)+DBTFD(J+1))/2.
006204          IF(DBTFD(J).LE.DMAX) GO TO 6958
006207          DMAX=DBTFD(J)
006210          TMAX=THSTFD(J)
006212     6958 CONTINUE
          *
          C     NORMALIZE DBTFD
006214          DO 6959 J=1,180
006216          DBTFD(J)=DBTFD(J)-DMAX
006220          IF(DBTFD(J).LT.-40.) DBTFD(J)=-40.
006224     6959 CONTINUE
006226          PRINT 5554,DMAX,TMAX
006236     5554 FORMAT(///* MAX DBTFD=*F9.5* FOR THSTFD=*F3* DEG*)
006236          PRINT 5555,(THSTFD(J),DBTFD(J),J=1,180)
006252     5555 FORMAT(//* THSTFD*7X*DBTFDNOR*/(2XF3,8XF10.5))
          *
006252          CALL POLPLT(THSTFD,DBTFD,180,7.5,8,1,N,TYPE,AL,XLAMDA,X,XL,H,RI,RS
               1,THI,DMAX,FIELD,SOURCE)
006275          PRINT 8888
006301     8888 FORMAT(///)
          *
006301          CALL TEST(N,AL,RS+RI,A,TYPE,SOURCE)
006307          GO TO 6789
006310     1112 CONTINUE
006310          CALL CALPLT(0.,0.,999)
006313          STOP
006315          END
```

```
                    SUBROUTINE DFRCF(D,XN,Y,B,XLMCA)
              C
              C     THIS ROUTINE IS TO COMPUTE THE DIFFRACTION COEFFICIENT
              C
 000010             COMPLEX F1J,F2J,G,R,T1,D1,T2,D2,D,F1,F2,S
              C
 000010             COMMON/PICONST/PI,TWOPI,STP,SQRTPI,TT,TTDEG,PIO2,PIO4
              *
 000010             BR=B*TT
 000011             ARG1=(PI+BR)/(2.0*XN)
 000015             ARG2=(PI-BR)/(2.0*XN)
 000020             CX1=COS(ARG1)
 000022             CX2=COS(ARG2)
 000024             SX1=SIN(ARG1)
 000026             SX2=SIN(ARG2)
 000030             X1=(BR+PI)/(2.0*XN*PI)
 000037             N1=X1
 000041             E1=X1-N1
 000043             IF(E1.GT.0.5) N1=N1+1
 000050             IF(E1.LT.-0.5) N1=N1-1
 000054             FN1=FLOAT(N1)
 000055             X2=(BR-PI)/(2.0*XN*PI)
 000061             N2=X2
 000063             E2=X2-N2
 000065             IF(E2.GT.0.5) N2=N2+1
 000072             IF(E2.LT.-0.5) N2=N2-1
 000076             FN2=FLOAT(N2)
 000077             A1=1.0+COS(-BR+2.0*XN*PI*FN1)
 000113             A2=1.0+COS(-BR+2.0*XN*PI*FN2)
 000127             SA1=SQRT(A1)
 000131             SA2=SQRT(A2)
 000133             XX=(SQRT( TWOPI*Y))*SA1
 000146             YY=(SQRT( TWOPI*Y))*SA2
 000156             XXS=XX*XX
 000160             YYS=YY*YY
 000161             PQ=SQRT(PIO2)
 000154             CALL CS(C1,S1,XXS)
 000166             CC1=0.5-C1
 000170             SS1=0.5-S1
 000172             F1J= PQ*CMPLX(SS1,CC1)
 000202             CALL CS(C2,S2,YYS)
 000205             CC2=0.5-C2
```

```
000207          SS2=0.5-S2
000211          F2J= PQ*CMPLX(SS2,CC2)
000221          P=-PI04
000222          Q=CMPLX(0.0,P)
000225          R=CEXP(Q)
000227          S=(-0.25*R*SQRT(XLMDA))/(PI*XN)
000254          T1=S*2.0*CEXP(CMPLX(0.0,XXS))
000270          D1=T1*F1J*CX1*(XX/SX1)
000302          T2=S*2.0*CEXP(CMPLX(0.0,YYS))
000316          D2=T2*F2J*CX2*(YY/SX2)
000330          D= D1+D2
000340          RETURN
000341          END

                SUBROUTINE KKDC(D,XN,XL,PHIP,PHI,XLMDA,T)
          C     D      - KARP - KELLER DIFFRACTION COEFFICIENT
          C     XL     - DISTANCE PARAMETER IN ANY UNIT
          C     XLMDA  - WAVELENGTH IN THE SAME UNIT
          C     PHIP   - ANGLE OF INCIDENCE IN DEGREES
          C     PHI    - ANGLE OF OBSERVATION IN DEGREES
          C     XN     - WEDGE ANGLE = (2.-XN)*PI
          C     T      - D/D(PHIP) OR D/D(PHI) = 1 OR 0
000012          INTEGER T
000012          COMPLEX D,D1,D2
000012          BETAP=PHI+PHIP
000013          BETAM=PHI-PHIP
000015          CALL CD(D1,XN,XL,BETAP,XLMDA, 1   ,T)
000022          CALL CD(D2,XN,XL,BETAM,XLMDA,-1   ,T)
000033          D=D2-D1
000043          RETURN
000044          END
```

```
                 SUBRCUTINE CD(D,XN,XL,BETA,XLMCA,T1,T2)
        C        T1  - BETP OR BETM 1 OR -1
        C        T2  - C/D(PHIS) OR C/D(PHIO) 1 OR 0
000012           INTEGER T1,T2
000012           COMPLEX D,CP,CM,DP,DM,V,P,CCP,CCM,C,F1,F2
000012           P(X)=CEXP(CMPLX(.0,X))
        C
00003C           COMMON/PICONST/PI,TWCPI,STP,SQRTPI,TT,TTDEG,PIO2,PIO4
        *
000030           XK=TWOPI/XLMDA
000031           C=P(-PIO4 )/(4.*(XN**2)*SQRT(TWOPI*XK))
000053           BR=BETA*TT
000054           TP=(PI+BR)/(2.*XN)
000060           ATP=ABS(TP)
000062           IF(ATP .LT. 0.01)GO TO 10
000065           XNP=(BR+PI)/(2.*XN*PI)
000070           NP=XNP
000072           E1=XNP-NP
000074           IF(E1. GT.  0.5)NP=NP+1
000100           IF(E1 .LT. -0.5)NP=NP-1
000104           AP=1.+COS(-BR+2.*XN*NP*PI)
000120           XKAP=XK*XL*AP
000122           CP=CEXP(CMPLX(.0,-PIO4 ))/(4.*(XN**2)*SQRT(TWCPI*XK)*(SIN((PI+BR)/
                1(2.*XN))**2))
000155           CCP=CP*V(XKAP)
000175           GO TC 11
000201     10    A1=2.*XK*XL*(XN**2)*(ATP**2)
000207           CALL CS(C1,S1,A1)
000211           F1=CMPLX(.C,4.*XK*XL*(XN**2))+2.*SQRTPI   *P(A1)*((2.*XK*XL*(XN**2)
                1)**1.5)*ATP*(P(-PIC4 )-SQRT(2.)*CMPLX(C1,-S1))
000273           CCP=C*F1
000301     11    TM=(PI-BR)/(2.*XN)
000304           ATM=ABS(TM)
000306           IF(ATM .LT. 0.01)GO TO 20
000311           XNM=(BR-PI)/(2.*XN*PI)
000314           NM=XNM
000316           E2=XNM-NM
000320           IF(E2 .GT.  0.5)NM=NM+1
000324           IF(E2 .LT. -0.5)NM=NM-1
000330           AM=1.+COS(-BR+2.*XN*NM*PI)
000344           XKAM=XK*XL*AM
000346           CM=CEXP(CMPLX(.0,-PIO4 ))/(4.*(XN**2)*SQRT(TWOPI*XK)*(SIN((PI-BR)/
```

```
                1(2.*XN))**2))
000411           CCM=CM*V(XKAM)
000421           GO TO 21
000425    20     A1=2.*XK*XL*(XN**2)*(ATP**2)
000433           CALL CS(C1,S1,A1)
000435           F2=CMPLX(.0,4.*XK*XL*(XN**2))+2.*SQRTPI   *P(A1)*((2.*XK*XL*(XN**2)
                1)**1.5)*ATM*(P(-PI04 )-SQRT(2.)*CMPLX(C1,-S1))
000517           CCM=C*F2
000525    21     IF(T1 .EQ.  1  )GO TO 1
000527           DP=CCP
000531           DM=-CCM
000534           IF(T2 .EQ.  1  )DP=-CCP
000540           IF(T2 .EQ.  1  )DM=CCM
000545           GO TO 2
000546    1      DP=CCP
000551           DM=-CCM
000553    2      D=DP+DM
000560           RETURN
000561           END

                 COMPLEX FUNCTION V(X)
          C      TRANSITION FUNCTION FOR THE INTEGRAL WITH THE INTEGRAND HAVING THE
          C      POLE OF ORDER TWO CLOSE TO THE SADDLE
          C      X = K*A(BETA)
000003           COMPLEX P
000003           P(X)=CEXP(CMPLX(.0,X))
          C
000016           COMMON/PICONST/PI,    TP,STP,SQRTPI,TT,TTDEG,PID2,PID4
000016           CALL CS(C,S,X)
000021           V=CMPLX(.0,2.*X)+2.*(X**1.5)*P(X)*SQRTPI   *(P(-PID4 )-SQRT(2.)*
                1CMPLX(C,-S))
000071           RETURN
000073           END
```

```
              SUBROUTINE WANG(PH,PHP,XN,XL,D1,D2)
000011        COMPLEX   D1,D2,DA,DB,DH,DS,U,V
000011        DH(U,V)=SQRT(6.283185301796)*(U+V)
000036        DS(U,V)=SQRT(6.283185301796)*(U-V)
000052        CALL  DFRCF(DA,XN,XL,PH-PHP,1.0)
000067        CALL  DFRCF(DB,XN,XL,PH+PHP,1.0)
000077        D1=DH(DA,DB)
000111        D2=DS(DA,DB)
000120        RETURN
000121        END

              SUBROUTINE CS(C,S,X)
        C
        C          COMPUTES THE FRESNEL INTEGRALS
        C
        C       DESCRIPTION OF PARAMETERS
        C          C       THE RESULTANT VALUE C(X)
        C          S       THE RESULTANT VALUE S(X)
        C          X       THE ARGUMENT OF FRESNEL INTEGRALS
        C                  IF X IS NEGATIVE, THE ABSOLUTE VALUE IS USED
        C
        C          THE ARGUMENT VALUE X REMAINS UNCHANGED
        C
        C          C(X)=INTEGRAL(COS(T)/SQRT(2*LI*T) SUMMED OVER T FROM 0 TO X)
        C          S(X)=INTEGRAL(SIN(T)/SQRT(I*LI*T) SUMMED OVER T FROM 0 TO X)
        C
        C          EVALUATION
        C          USING DIFFERENT APPROXIMATIONS FOR X .LT. 4 AND X .GT. 4
        C
        C          REFERENCE
        C           COMPUTATION OF FRESNEL INTEGRALS  BY BOERSMA,
        C          MATHEMATICAL TABLES AND OTHER AIDS TO COMPUTATION, VOL. 14,
        C          1960, NO. 72, P. 380
        C
0006          Z=ABS(X)
0007          IF(Z-4.)1,1,2
0012        1 C=SQRT(Z)
0016          S=Z*C
0020          Z=(4.-Z)*(4.+Z)
0024          C=C*((((((5.100785E-11*Z+5.244297E-9)*Z+5.451182E-7)*Z
             1+3.273308E-5)*Z+1.020418E-3)*Z+1.102544E-2)*Z+1.840965E-1)
0037          S=S*(((((6.677681E-10*Z+5.883158E-8)*Z+5.051141E-6)*Z
             1+2.441816E-4)*Z+6.121320E-3)*Z+8.026490E-2)
```

```
0050            RETURN                                                                78400000
C051          2 D=COS(Z)                                                              78500000
0053            S=SIN(Z)                                                              78700000
C061            Z=4./Z                                                                78800000
0063            A=(((((((8.768258E-4*Z-4.169289E-3)*Z+7.970943E-3)*Z-6.792801E-3)      78900000
               1*Z-3.095341E-4)*Z+5.972151E-3)*Z-1.606428E-5)*Z-2.493322E-2)*Z         79000000
               2-4.444091E-9                                                          79100000
C100            B=((((((-6.633926E-4*Z+3.401409E-3)*Z-7.271690E-3)*Z+7.428246E-3)      79200000
               1*Z-4.027145E-4)*Z-9.314910E-3)*Z-1.207998E-6)*Z+1.994711E-1           79300000
0113            Z=SQRT(Z)                                                             79400000
000115          C=0.5+Z*(D*A+S*B)                                                     79500000
000125          S=0.5+Z*(S*A-D*B)                                                     79600000
000132          RETURN                                                                79700000
000133          END                                                                   79800000
```

```
                 SUBROUTINE TEST(N,AL,XS,A,TYPE)
          C THIS SUBROUTINE PROGRAM COMPUTES THE RADIATION FIELD OF HORN ANTENNA
          C
000010           DIMENSION X(180),AM(180),AP(180),DG(180),A(180),ANG(180)
000010           DIMENSION THIFD(185),AMPIFD(185),DBIFD(185)
000010           COMPLEX F,A,DG,CDG,TAL
000010           COMMON XLAMDA,XPIN,XL,H,RI,RS,THI,DMAX,FIELD,SOURCE
000010           COMMON/PICONST/PI,    TP,STP,SQRTPI,TT,TTDEG,PIO2,PIO4
          C        XPIN IS POINT OF INCIDENCE WHICH IS X IN MAIN PROGRAM
          C
000010           F(Z)=CEXP( CMPLX(0.,-6.2831853071796*Z))/SQRT(6.2831853071796*Z)
000036           FA(SA,SB,SC)= ACOS((SB*SB+SC*SC-SA*SA)/(2.0*SB*SC))
000057           FC(AA,SB,SC)=SQRT(SB*SB+SC*SC-2.0*SB*SC*COS(AA))
000101           FB(SX)=ABS(COS(SX/2.0))**2.0
          C
          C FB(SX) IS THE OBLIQUITY FACTOR.     TO IGNORE IT, SET FB(SX)=1.
          C
          *
000120           NN=(N+1)/2
000122           L=0
000123           D=0.0
000123           IF(N.GT.1) D=AL/FLOAT(N-1)
000130           TH=0.0
000131         2 CONTINUE
000131           IF(TH.EQ.90.0) GO TO 15
000133           THR=TH*TT
000134           ANG(1)=THR
000136           X(1)=XS
000137           DG(1)=A(1)*F(XS)*FB(THR)
000153           IF(TYPE.EQ.3.0.AND.THR.LT.PIO2   ) DG(1)=DG(1)*COS(THR)
000175           IF(TYPE.EQ.3.0.AND.THR.GT.PIO2   ) DG(1)=DG(1)*COS(PI-THR)
000221           IF(N.EQ.1) GO TO 11
000223           I=2
000224         3 CONTINUE
000224           X(I)=FC(PI*0.5+THR,FLOAT(I-1)*D,XS)
000236           IF(I.GT.NN) X(I)=FC(PIO2  -THR,FLOAT(I-NN)*D,XS)
000251           IF(TH.GT.90.0) X(I)=FC(1.5*PI-THR,FLOAT(I-1)*D,XS)
000266           IF(TH.GT.90..AND.I.GT.NN) X(I)=FC(THR-PIO2   ,FLOAT(I-NN)*D,XS)
000311           ANG(I)=THR+FA(FLOAT(I-1)*D,XS,X(I) )
000323           IF(I.GT.NN) ANG(I)=THR-FA(FLOAT(I-NN)*D,XS,X(I) )
000336           IF(TH.GT.90.0) ANG(I)=THR-FA(FLOAT(I-1)*D,XS,X(I) )
000352           IF(TH.GT.90.0.AND.I.GT.NN) ANG(I)=THR+FA(FLOAT(I-NN)*D,XS,X(I) )
```

```
000376          DG(I)=A(I)*F(X(I))*FB(ANG(I) )
000416          IF(TYPE.EQ.3.0.AND.ANG(I).LT.PIO2   ) DG(I)=DG(I)*COS(ANG(I))
000442          IF(TYPE.EQ.3.0.AND.ANG(I).GT.PIO2   ) DG(I)=DG(I)*COS(PI-ANG(I))
000470          IF(I.EQ.N) GO TO 11
000472          I=I+1
000473          GO TO 3
000474       11 CONTINUE
000474          TAL=CMPLX(0.0,0.0)
000477          DO 33  K=1,N
000500          CDG=DG(K)
000503          ANGL=ANG(K)*TTDEG
000505          ADG=CABS(CDG)
000507          TAL=TAL+DG(K)
000516       33 CONTINUE
000523          ATAL=CABS(TAL)
000524          IF(TH.EQ.0.0) XNCM=ATAL
000532          DBTAL=20.0*ALOG10(ATAL)
000536          WRITE(6,4) TH,ATAL,DBTAL
000547        4 FORMAT(    5X*TH=*F10.4,5X,*MAGNITUDE= *,E15.4,5X,*DBHA= *,E15.4)
000547          L=L+1
         *
000551          THIFD(L)=TH
000553          AMPIFD(L)=ATAL
000554          DBIFD(L)=DBTAL
000556       15 CONTINUE
000556          TH=TH+2.0
000560          IF(TH.LE.360.0) GO TO 2
000566          PRINT 39,(THIFD(J),AMPIFD(J),DBIFD(J), J=1,L)
000604       39 FORMAT(///2X* TH*7X*AMPLITUDE*7X* DBHA*/(F5,2(5XF10.5)))
         C    FIND MAX AMPIFD
000604          AMAX=AMPIFD(1)
000605          TMAX= THIFD(1)
000607          DO 6596 J=2,L
000614          IF (AMPIFD(J).LE.AMAX) GO TO 6596
000617          AMAX=AMPIFD(J)
000620          TMAX= THIFD(J)
000621     6596 CONTINUE
         C    NORMALIZE AMPIFD
000624          DO 6597 J=1,L
000625          AMPIFD(J)=AMPIFD(J)/AMAX
000627     6597 CONTINUE
000631          PRINT 5555,AMAX,TMAX
000641     5555 FORMAT(//* MAX AMPIFD=*F9.5,* FOR THIFD=*F3* DEG*)
```

```
           **     IN TEST
           *
 )0641            FIELD=5HINCID
 )0642            DMAX=DBIFD(1)
 )0644            TMAX=THIFD(1)
 )0646            DO 6598 J=2,L
 )0652            IF(DBIFD(J).LE.DMAX) GO TO 6598
 )0655            DMAX=DBIFD(J)
 )0656            TMAX=THIFD(J)
 )0657       6598 CONTINUE
           C   NORMALIZE DBFA WHICH IS DBIFD
 )0662            DO 6599 J=1,L
 )0663            DBIFD(J)=DBIFD(J)-DMAX
 )0665            IF(DBIFD(J).LT.-40.) DBIFD(J)=-40.
 )0671       6599 CONTINUE
 )0674            PRINT 5556,DMAX,TMAX
 )0703       5556 FORMAT(///* MAX DBIFD=*F9.5* FOR THIFD=*F3* DEG*)
 )0703            PRINT 40,(THIFD(J),AMPIFD(J),DBIFD(J), J=1,L)
 )0722         40 FORMAT(//* THIFD*5X*AMPIFDNOR*7X*DBIFDNOR*/(F5,2(4XF10.5)))
 )0722            CALL POLPLT(THIFD,DBIFD, 180,7.5,8,1,N,TYPE,AL,XLAMDA,XPIN,XL,H,RI
                 1,RS,THI,DMAX,FIELD,SOURCE)
           ***
 )0751            THIFD(L+1)=0.
 )0753            THIFD(L+2)=30.
 )0754            AMPIFD(L+1)=0.
 )0755            AMPIFD(L+2)=.1
 )0757            CALL PLTIFD(THIFD,AMPIFD,180)
 )0761            RETURN
 )0762            END

                  SUBROUTINE PLTTFD(THSTFD,AMPTFD,NPTS)
000006            DIMENSION THSTFD(1),AMPTFD(1)
000006            TMAJ=1.
000007            TMIN=3.
000011            CALL NOTATE(0.00,0.2,.28,11HTOTAL FIELD,0.,11)
000015            CALL CALPLT(0.,1.0,-3)
000021            CALL AXES(0.,0.,90.,10.,0.,0.1,1.,5.,9HAMPLITUDE,.28,9)
000033            CALL AXES(0.,0.,0.,12.,-180.,30.,TMAJ,TMIN,10HTHSTFD,DEG,.28,-10)
000046            CALL AXES(0.,10.,0.,12.,   0.,30.,TMAJ,TMIN,1H ,0.,1)
000061            CALL AXES(12.,0.0,90.,10.,0.,0.1,1.,5.,1H ,0.,-1)
000074            CALL LINE(THSTFD,AMPTFD,NPTS,1,0,0,0.)
000103            CALL NFRAME
000104            RETURN
000105            END
```

```
SUBROUTINE PLTTFDP(THSTFD,PHTFD,NPTS)
DIMENSION THSTFD(1),PHTFD(1)
TMAJ=1.
TMIN=3.
CALL NOTATE(0.00,0.2,.28,11HTOTAL FIELD,0.,11)
CALL CALPLT(0.,1.0,-3)
CALL AXES(0.,0.,90.,12.,-180.,30.,1.,3.,9HPHASE,DEG,.28,9)
CALL AXES(0.,0.,0.,12.,-180.,30.,TMAJ,TMIN,10HTHSTFD,DEG,.28,-10)
CALL AXES(0.,12.,0.,12.,-180.,30.,TMAJ,TMIN,1H ,0.,1)
CALL AXES(12.,0.0,90.,12.,-180.,30.,1.,3.,1H ,0.,-1)
CALL LINE(THSTFD,PHTFD,NPTS,1,0,0,0.)
CALL NFRAME
RETURN
END
```

```
              SUBROUTINE PULPLT(DEGS,DBS,NPTS,DIAM,NOCIR,NPLOTS,N,TYPE,AL,
             1XLAMDA,X,XL,H,RI,RS,THI,DMAX,FIELD,SOURCE)
       *
0026          DIMENSION DEGS(1),DBS(1),CHTAB(16)
C026          DIMENSION ANUM(11),FIELD(2)
0026          DIMENSION CCB(400),RHOX(400),RHOY(400),PHI(400)
       *
0026          RAD  =DIAM/2.0
C027          HGT=.21
       *
0031          CHTAB(1)  =1H
0032          CHTAB(2)  =1H5
0034          CHTAB(3)  =2H10
0035          CHTAB(4)  =2H15
C037          CHTAB(5)  =2H20
0040          CHTAB(6)  =2H25
0042          CHTAB(7)  =2H30
C043          CHTAB(8)  =2H35
       *
       *
0045          CALL NOTATE (0.,0.,HGT,3,0.,-1)
0051          RADO =RAD
0052          DELTR=RAD/NOCIR
C060          CX=10.
C061          PX=10.
0062          AY= 5.0
C063          PY=5.
0064          K=1
0065          HGT=.14
       *
C067        1 CONTINUE
0067          DO 5 I=1,NOCIR
C071          RADF=RADO
0073          CALL CIRCLE(CX ,AY,0.,360.,RADO,RADF,3)
C101          IF(I.EQ.3)K=2
C110          CALL NOTATE (CX,AY,HGT,CHTAB(I),270.,K)
0116          RADO=RADO-DELTR
0120          CX= CX-DELTR
0121        5 CONTINUE
       ***  CORDINATES FOR CENTER CF CIRCLE  ****
0127          CNTRX=PX-RAD
0130          CNTRY=PY
```

```
000132         ANGLE=.174532925
000133         TIC=.1
000135         RPT=RAD+TIC
000136         DELTA=.174532925
        *
        ***    DRAW TIC MARKS EVERY 10 DEGREES    ***
        *
000140         DO 50 I=1,36
        ***    PAGE COORDINATES    ***
000141         TICX1=CNTRX+RAD*COS(ANGLE)
000145         TICY1=CNTRY+RAD*SIN(ANGLE)
000152         TICX2=CNTRX+RPT*COS(ANGLE)
000157         TICY2=CNTRY+RPT*SIN(ANGLE)
000164         CALL CALPLT(TICX1,TICY1,3)
000167         CALL CALPLT(TICX2,TICY2,2)
000172         ANGLE=ANGLE+DELTA
000174      50 CONTINUE
        *
        *** DRAW LABLES ***
        *
000202         ANUM(1)=N
000203         ANUM(2)=TYPE
000205         ANUM(3)=AL
000206         ANUM(4)=XLAMDA
000210         ANUM(5)=X
000211         ANUM(6)=XL
000213         ANUM(7)=H
000214         ANUM(8)=RI
000216         ANUM(9)=RS
000217         ANUM(10)=THI/(.1*DELTA)
000222         ANUM(11)=DMAX
000224         CALL NOTATE(11.40,9.0,.21,14HTRANSMITED WL=,270.,14)
000230         CALL NUMBER(11.40,6.5,.21,ANUM(4),270.,-1)
000236         CALL NOTATE(11.40,4.3,.21,12HINCID RANGE=,270.,12)
000242         CALL NUMBER(11.40,2.0,.21,ANUM(8),270.,2)
000250         CALL NOTATE(11.10,9.0,.21,12HINCID POINT=,270.,12)
000254         CALL NUMBER(11.10,6.7,.21,ANUM(5),270., 2)
000262         CALL NOTATE(11.10,4.3,.21,12HSCATER RNGE=,270.,12)
000266         CALL NUMBER(11.10,2.0,.21,ANUM(9),270.,-1)
000274         CALL NOTATE(10.80,9.0,.21,11HBOX LENGTH=,270.,11)
000300         CALL NUMBER(10.80,6.9,.21,ANUM(6),270.,2)
000306         CALL NOTATE(10.80,4.3,.21,12HINCID ANGLE=,270.,12)
000312         CALL NUMBER(10.80,2.0,.21,ANUM(10),270.,-1)
```

```
000320        CALL NOTATE(10.50,9.0,.21,11HBOX HEIGHT=,270.,11)
000324        CALL NUMBER(10.50,6.9,.21,ANUM(7),270.,-1)
000332        CALL NOTATE(10.50,4.3,.21,12HNORMALIZ D3=,270.,12)
000336        CALL NUMBER(10.50,2.0,.21,ANUM(11),270.,3)
000344        CALL NOTATE( 1.70,4.3,.21,15HLINE SOURCES,N=,270.,15)
000350        CALL NUMBER( 1.70,1.6,.21,ANUM(1),270.,-1)
000356        CALL NOTATE( 1.40,4.8,.21,20H       CURNT TYPE=,270.,20)
000362        CALL NUMBER( 1.40,1.2,.21,ANUM(2),270.,-1)
000370        CALL NOTATE( 1.40,4.8,.21,SOURCE,270.,9)
000375        CALL NOTATE(1.10,9.0,.21,11H      FIELD,270.,11)
000401        CALL NOTATE(1.10,9.0,.21,FIELD,270.,5)
000406        CALL NOTATE( 1.10,4.0,.21,12HAPERT WIDTH=,270.,12)
000412        CALL NUMBER(1.10,1.75,.21,ANUM(3),270.,3)
        *** DRAW X AXIS
000420        AX=PX-DIAM-.5
000427        CALL CALPLT(AX,AY,3)
000431        AX=PX+.5
000433        CALL CALPLT(AX,AY,2)
        *** DRAW ZERO DEGREES AFTER HORIZONTAL
000436        HGT=.21
000437        AX=PX
000441        AY=AY-.05
000443        CALL NOTATE (AX,AY,HGT,1H0,270.,1)                DEGREES
000447        AX=AX+.21
000451        AY=AY-.12
        *** DEGREE SYMBOL
000453        CALL NOTATE (AX,AY,.07,1H0,270.,1)
        ***DRAW Y AXIS
000457        AY=5.0
000460        AX= PX-RAD
000462        AY= AY-RAD-.5
000466        CALL CALPLT(AX,AY,3)
000470        AY=AY+ DIAM+1.
000476        CALL CALPLT(AX,AY,2)                              VERTICAL
        ***DRAW 90 DEGS
000501        AY=AY-.1
000503        CALL NOTATE(AX,AY,HGT,2H90,270.,2)
000507        AX=AX+HGT
000511        AY=AY-.32
000513        CALL NOTATE (AX,AY,.07,1H0,270.,1)
        *** DRAW 180 DEGREES
000517        AX=PX-DIAM-.3
000525        AY=5.0
```

```
000527           CALL NCTATE (AX,AY,HGT,3H180,270.,3)
000533           AX=AX+.21
000535           AY=AY-.5
COC537           CALL NOTATE (AX,AY,.07,1HO,270.,1)
        *
        ***DRAW 270 DEGS
000543           AX=PX-RAD
000545           AY=5.0-RAD-.05
000550           CALL NCTATE(AX,AY,HGT,3H270,270.,3)
000554           AX=AX+HGT
000556           AY=AY-.5
000560           CALL NCTATE (AX,AY,.07,1HO,270.,1)
        *
        **
        *
000554      151 CONTINUE
        *
        *** PLOT POLAR CURVES ***
        *
        *** SCALE DECIBELS AND CONVERT POLAR COORDINATES TO CART. COORDS.
00C564           DO 500 JJ=1,NPTS
000571           PHI= DEGS(JJ)*.0174532925
00C573           CCB(JJ)=DBS(JJ)+40.
000576           CDB(JJ)=.025*RAD*CDB(JJ)
000601           RHOX(JJ)=CDB(JJ)*COS(PHI      )+PX-RAD
00C610           RHOY(JJ)=CDB(JJ)*SIN(PHI      )+5.0
000616      500 CONTINUE
000624           LIM=NPTS-1
        ***BEGIN PLOTTING WITH PEN UP***
000625           IPEN=3
000627           DO 100 I=1,LIM
000630           J=I+1
000632           CALL CIRCLE(RHOX(I),RHOY(I),DEGS(I),DEGS(J),CDB(I),CDB(J),IPEN)
000655           IF(I.GT.1)GO TO 110
000664           IPEN=2
000655      110 CONTINUE
000665      100 CONTINUE
        *
000670           CALL NFRAME
000671           RETURN
000672           END
```

```
                SUBROUTINE PLTIFD(THIFD,AMPIFD,NPTS)                                111000000
000005          DIMENSION THIFD(1),AMPIFD(1)                                        111100000
000006          TMAJ=1.                                                             111200000
000007          TMIN=3.                                                             111300000
000011          CALL NOTATE(0.00,0.2,.28,14HINCIDENT FIELD,0.,14)                   111400000
000015          CALL CALPLT(0.,1.0,-3)                                              111500000
000025          CALL AXES(0.,0.,90.,10.,0.,0.1,1.,5.,9HAMPLITUDE,.28,9)             111600000
000033          CALL AXES(0.,0.,0.,12.,0.,30.,TMAJ,TMIN,9HTHIFD,DEG,.28,-9)         111700000
000046          CALL AXES(0.,10.,0.,12.,-180.,30.,TMAJ,TMIN,1H ,0.,1)               111800000
000061          CALL AXES(12.,0.0,90.,10.,0.,0.1,1.,5.,1H ,0.,-1)                   111900000
000074          CALL LINE(THIFD,AMPIFD,180,1,0,0,0.)                                112000000
000104          CALL NFRAME                                                         112100000
000105          RETURN                                                              112200000
000106          END                                                                 112300000
```

REFERENCES

1. Keller, J. B., "Geometrical Theory of Diffraction," J. Opt. Soc. Am., 52, pp. 116-130, 1962.

2. Meil, K. K. and Van Bladel, J. G., "Scattering by Perfectly-Conducting Rectangular Cylinders," IEEE Trans, AP-11, pp. 185-192, 1963.

3. Andreasen, M. G. and Mei, K. K., "Scattering by Conducting Cylinders," IEEE Trans, AP-12, pp. 235-236, 1964.

4. Morse, B. J., "Diffraction by Polygonal Cylinders," J. Math. Phys., 5, pp. 199-214, 1964.

5. Oberhettinger, F., "On Asymptotic Series for Functions Occurring in the Theory of Diffraction of Waves by Wedges," J. Math. Phys., 34, pp. 245-255, 1956.

6. Pathak, P. H. and Kouyoumjian, R. G., "The Dyadic Diffraction Coefficient for a Perfectly-Conducting Wedge." Report 2183-4, June 1970, The Ohio State University ElectroScience Laboratory, Department of Electrical Engineering; prepared under Contract AF 19(628)-5929 for Air Force Cambridge Research Laboratories. (AFCRL-69-0546) (AD 707 827)

7. Kouyoumjian, R. G. and Pathak, P. H., "The Dyadic Diffraction Coefficient for a Curved Edge." NASA CR-2401, 1974.

8. Karp. S. N. and Keller, J. B., "Multiple Diffraction by an Aperture in a Hard Screen," Optica Acta, 8, pp. 61-72, 1961.

NATIONAL AERONAUTICS AND SPACE ADMINISTRATION
WASHINGTON, D.C. 20546

OFFICIAL BUSINESS
PENALTY FOR PRIVATE USE $300

SPECIAL FOURTH-CLASS RATE
BOOK

POSTAGE AND FEES PAID
NATIONAL AERONAUTICS AND
SPACE ADMINISTRATION
451

U.S.MAIL

POSTMASTER: If Undeliverable (Section 158 Postal Manual) Do Not Return

"The aeronautical and space activities of the United States shall be conducted so as to contribute . . . to the expansion of human knowledge of phenomena in the atmosphere and space. The Administration shall provide for the widest practicable and appropriate dissemination of information concerning its activities and the results thereof."

—NATIONAL AERONAUTICS AND SPACE ACT OF 1958

NASA SCIENTIFIC AND TECHNICAL PUBLICATIONS

TECHNICAL REPORTS: Scientific and technical information considered important, complete, and a lasting contribution to existing knowledge.

TECHNICAL NOTES: Information less broad in scope but nevertheless of importance as a contribution to existing knowledge.

TECHNICAL MEMORANDUMS: Information receiving limited distribution because of preliminary data, security classification, or other reasons. Also includes conference proceedings with either limited or unlimited distribution.

CONTRACTOR REPORTS: Scientific and technical information generated under a NASA contract or grant and considered an important contribution to existing knowledge.

TECHNICAL TRANSLATIONS: Information published in a foreign language considered to merit NASA distribution in English.

SPECIAL PUBLICATIONS: Information derived from or of value to NASA activities. Publications include final reports of major projects, monographs, data compilations, handbooks, sourcebooks, and special bibliographies.

TECHNOLOGY UTILIZATION PUBLICATIONS: Information on technology used by NASA that may be of particular interest in commercial and other non-aerospace applications. Publications include Tech Briefs, Technology Utilization Reports and Technology Surveys.

Details on the availability of these publications may be obtained from:

SCIENTIFIC AND TECHNICAL INFORMATION OFFICE

NATIONAL AERONAUTICS AND SPACE ADMINISTRATION

Washington, D.C. 20546